



MINISTRY OF  
CLIMATE AND ENERGY

**enviroRISKS**

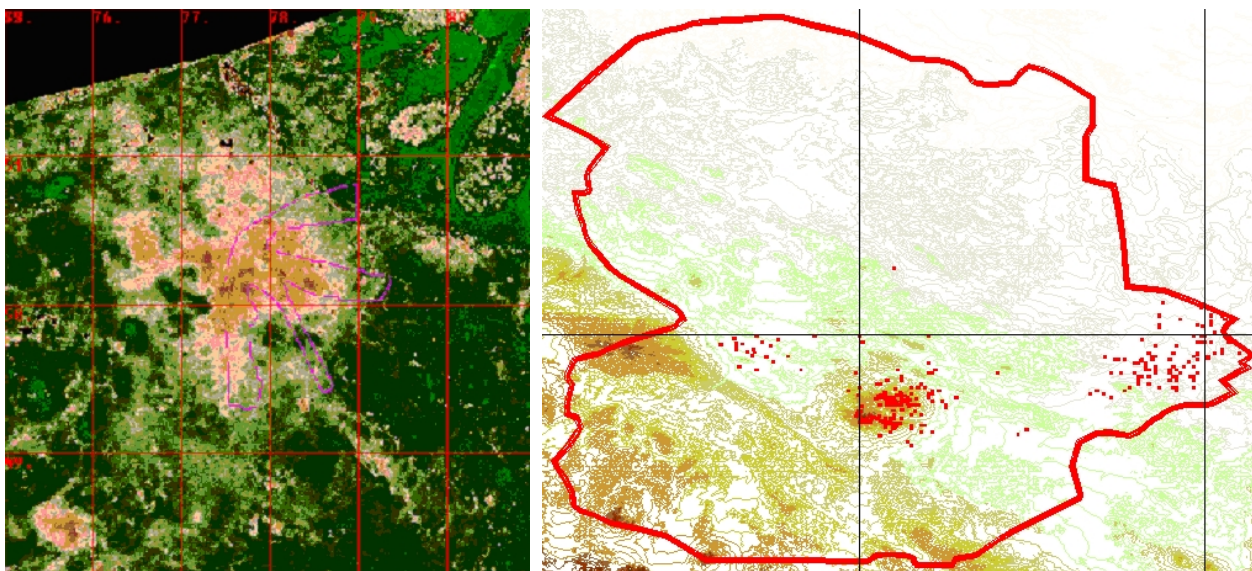


## Scientific Report 08-06

# Geoinformation Modeling of Radionuclide Transfer from the Territory of the Semipalatinsk Test Site

Edige Zakarin, Larissa Balakay, Bibigul Mirkarimova, Natalia Tuseeva, Konstantin Pak, Alexander Baklanov, Alexander Mahura, Jens H. Sorensen

FP6 EC CA - Enviro-RISKS: Man-induced Environmental Risks: Monitoring, Management and Remediation of Man-made Changes in Siberia



Copenhagen 2008



## Colophon

**Serial title:**

Scientific Report 08-06

**Title:**

Geoinformation Modeling of Radionuclide Transfer from the Territory of the Semipalatinsk Test Site

**Subtitle:**

FP6 EC CA - Enviro-RISKS: Man-induced Environmental Risks: Monitoring, Management and Remediation of Man-made Changes in Siberia

**Author(s):**

Edige Zakarin, Larissa Balakay, Bibigul Mirkarimova, Natalia Tuseeva, Konstantin Pak, Alexander Baklanov, Alexander Mahura, Jens H. Sorensen

**Responsible institution:**

Danish Meteorological Institute

**Language:**

English

**Keywords:**

Semipalatinsk Test Site, nuclear devices testing, thermal anomaly, object-oriented analysis, RUN-OFF, surface water modelling DERMA, atmospheric modelling, radionuclide caesium-137, GIS integration, MigRad

**Url:**

[www.dmi.dk/dmi/sr08-06.pdf](http://www.dmi.dk/dmi/sr08-06.pdf)

**Digital ISBN:**

978-87-7478-572-9

**ISSN:**

1399-1949

**Version:**

**Website:**

[www.dmi.dk](http://www.dmi.dk)

**Copyright:**



## Content:

Abstract .....	4
Introduction.....	5
1. Statement of the Problem.....	5
1.1. Semipalatinsk test site.....	5
1.2. Nuclear devices testing .....	6
1.3. Thermal anomaly on the test site territory .....	6
1.4. Tasks of MigRad project.....	7
2. Object-Oriented Analysis of the Studied Area .....	8
2.1. General interaction diagram.....	8
2.2. Diagram of classes .....	9
2.3. Sequence diagram .....	9
2.4. Database structure .....	10
3. Modeling of Radionuclides Migration with Surface Waters .....	12
3.1. RUNOFF Model: basics and equations .....	12
3.2. Structure of model and data flow .....	14
3.3. Modeling results.....	16
4. Mapping of High Temperature Zones on the Territory of Semipalatinsk Test Site .....	18
5. Mapping of Epicenters of Radioactive Aerosol Transport .....	19
6. Transboundary Atmospheric Transport of Radioactive Substances.....	20
6.1. DERMA Model: basics and equations.....	21
6.2. Input meteorological dataset .....	27
6.3. Selected assumptions for long-term simulations .....	28
6.4. Post-processing of concentration and deposition fields.....	29
6.5. Integration of modelling results into GIS environment .....	30
Conclusions.....	33
References.....	34
Appendix A: Radioactive pollution from Delegen test site .....	37
Appendix B: Radioactive pollution from Experimental Field test site.....	39



## **Abstract**

In this study we developed, tested and applied the software complex as the GIS-project MigRad (Migration of Radionuclide) oriented at integration of a large volume of various information (mapping, ground-based and satellite-based survey) and modeling on its base local redistribution of radionuclides by rain flows and long-range transfer of radioactive aerosol from the territory of the Semipalatinsk test site/ polygon (Republic of Kazakhstan). Since 1961, in total 348 underground nuclear explosions were made on the territory of the test site. The thermal anomaly on territory of the polygon was investigated, and the object-oriented analysis was employed for the studied area.

Employing the RUNOFF model, the simulation of radionuclides migration with surface waters was performed. Employing the DERMA model, the simulation of long-term atmospheric transport dispersion and deposition patterns for cesium was conducted from 3 selected test sites (Balapan, Delegen, and Experimental Field) was conducted. Employing GIS technology, the mapping of the of the high temperature zones and epicenters of radioactive aerosol transport for the territory of the test site was carried out with post-processing and integration of modelling results into GIS environment. Contamination levels of pollution due to former nuclear explosions for population and environment of the surrounding polygon areas of Kazakhstan as well as adjacent countries were analyzed and evaluated.

## Introduction

Over a long period of time the territory of the Semipalatinsk Test Site, STS (Figure 1) created in 1947 was subjected to extremely hard loads in the form of numerous tests of nuclear weapons. The consequences of such impact turned out to be very serious (*Sultangazin et al., 1998; Dubasov, 1997; Tleubergenov, 1997; Henson, 1985*) and will probably reveal themselves over a long period of time. The last test on the STS was carried out in October 1989 but still the level of radiation on the test site is much higher than the background values. Under the action of water and wind soil erosion radioactive substances are redistributed over the territory of the STS and spread beyond its boundaries. The people, living in the areas located close to the STS territory and rather far from it, eat vegetable and animal products contaminated with radionuclides, consume external irradiation and, thus, are subjected to the risk of radiation pollution.

The objective of this research is to develop a software complex as GIS-project MigRad (Migration of Radionuclide) oriented at integration of a large volume of various information (mapping, ground-based and satellite-based survey) and modeling on its base local redistribution of radionuclides by rain flows and long-range transfer of radioactive aerosol from the territory of the test site.

## 1. Statement of the Problem

Radiological situation and dynamics of its change on the territory of the test site and in the affected zones are formed under the action of a number of factors. Among them the most important are the areas of localization of test explosions, climatic characteristics of the region, properties of underlying surface and explosion-initiated processes.

### 1.1. Semipalatinsk test site

The test site under investigation is situated at the intersection of three oblasts (regions): Pavlodar, Karaganda and North-Kazakhstan oblasts (Figure 1), it stretches from 49°N, 77°E to 51°N, 79.5°E, its area is more than 18000 km<sup>2</sup>.

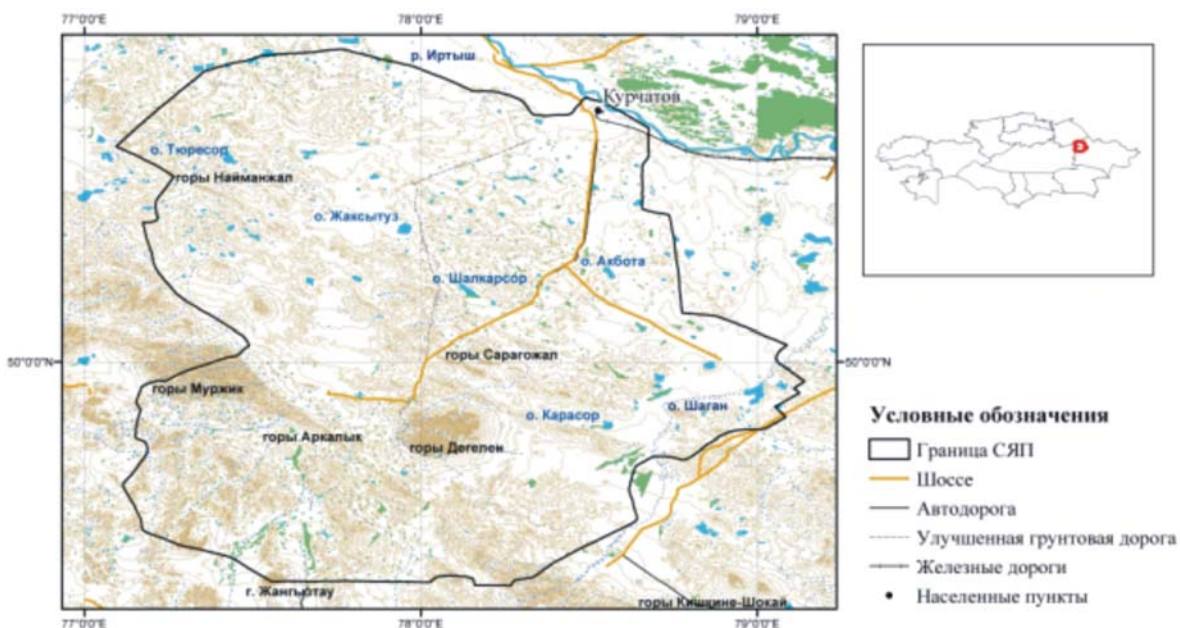


Figure 1. Semipalatinsk test site.

The climate of the test site is sharply continental with high daily and annual variations of air temperature (*Atlas, 1997; Logachev, 1997*). Winter is cold. The average temperature in January is as low as minus 20°C. Summer is long, hot and dry. The average temperature in July is +24°C. The annual

amount of precipitations ranges from 160 to 400 mm. In general, the territory of the test site refers to the area of insufficient and unstable moistening. A specific feature of the area is summer precipitations in the form of showers. Winds blow in different directions. Sometimes the wind changes its direction several times a day. The area is characterized by spring winds of westerly direction. In winter snow storms often blow. In warm seasons dust storms are observed. In summer winds are less strong. The area has scarce vegetation.

According to the relief structure the studied area refers to the low-hill type. It is characterized by alternating of hill chains and isolated ranges of low mountains (Delegen – 1085m, Murzhik – 601m) with vast valleys. The area has different types of soil cover. In the north, on the right bank of the Irtysh river, the soil can be classified as fixed by trees sands. The flood-lands of the Chagan and Atschisu are formed by solonetztes and solonchaks. Valleys and low-hill areas have light chestnut normal and solonetzic soils alternating with solonetztes. They are characterized by low profile, crushed-stone structure and small humus content (1.5 – 2 %). The above types of soils give scarce vegetation cover. Based on the above natural characteristics of the Test Site one can make a conclusion that the main mechanisms of radionuclide migration are connected with water (due to rains) and wind soil erosion.

## 1.2. Nuclear devices testing

In the period from 1949 to 1962 118 aboveground nuclear tests were made on the STS territory, 30 of them were surface nuclear tests, 5 of which were prepared but not exploded because of non-operation of nuclear devices (Tleubergenov, 1997). Since 1961, 348 underground nuclear explosions were made on the STS territory. The underground explosions were made both in horizontal tunnels (215 explosions) and in vertical wells (133 explosions) where nuclear explosive devices were placed (Tleubergenov, 1997). Information about nuclear explosions as a map where dots show the places of expositions is given below (Figure 2).

## 1.3. Thermal anomaly on the test site territory

One of the factors imposing strong influence on the formation of the epicenters of wind erosion is anomaly high temperature of the underlying surface. It was discovered using remote sensing data (Sultangazin et al., 1997; Zakarin et al., 1998). Satellite-based images of the STS territory obtained since 1997 show clearly outlined heat epicenters whose temperature by 7-10 degrees exceeds the average background temperature of surrounding area. This effect is especially clearly identified at the end of summer – beginning of spring. In this period snow cover on the test site melts earlier than on the surrounding areas, which is clearly seen on the photographs in visible light (Figure 3).

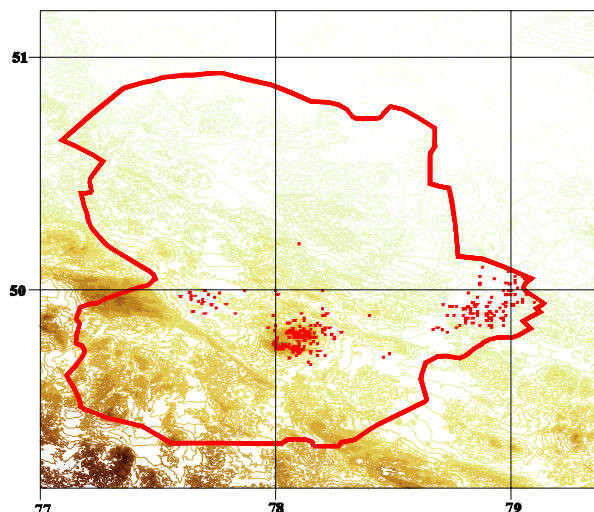
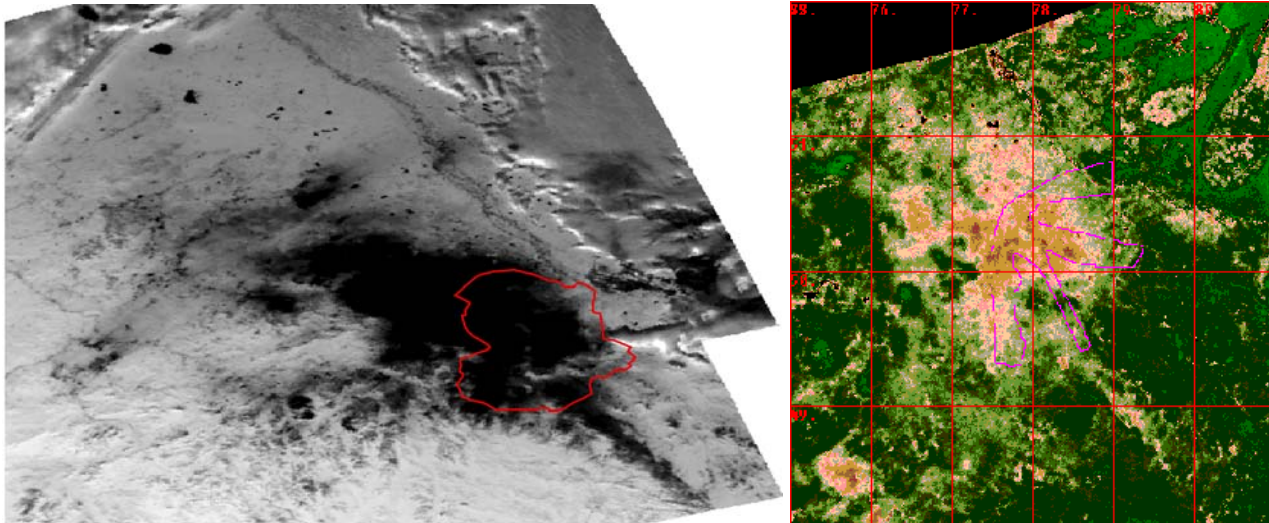


Figure 2. The places of nuclear explosions in Semipalatinsk test site territory.



**Figure 3.** Satellite-based image NOAA/AVHRR 17.02.1997 of the SPS territory. **Figure 4.** Areas on the STS not covered with vegetation. Satellite-based image NOAA/AVHRR, May 2, 1997.

This effect completely suppresses vegetation growth in dry years (Sultangazin et al., 1997), which is demonstrated by NDVI fields (Figure 4). Anomaly high temperatures were first registered during ground-based measurements of the temperature of underlying surface before and after the explosion. Investigations carried out by Busygin and his coworkers (Zakarin & Balakay, 2003) showed that in the recoil zone of an underground nuclear explosion temperature increased by 10 – 12<sup>0</sup>C and such overheating remained after explosion during all period of observations (over 20 years). According to the remote sensing data areas of anomalous zones vary from year to year, but all they have a common area including the test site. Processing of remote sensing data in thermal range enables to construct maps of temperature fields and to determine the value of overheating and configuration of heat areas for all period of observations. Independent of the reasons, which influenced formation of thermal anomalies, high temperature and absence of vegetation give rise to more intensive deflation processes in soil and as a result wind transfer of radioactive substances from its surface.

#### 1.4. Tasks of MigRad project

Based on the above-described territorial processes, let's identify the most important processes in terms of their impact on population. From our point of view such processes include transfer of radionuclides by surface waters to the closely-located areas and long-range transfer of radioactive aerosols to the territory of Kazakhstan and neighboring states.

Scientifically-based and visual studying of the above processes can be attained only on the base of geoinformation modeling (Turganbayev & Kazamirchuk, 1999a; Zakarin & Balakay, 2002). The above statement defines objective of the research – development of GIS-project MigRad uniting the base of territorially distributed data, modeling and methods of space monitoring (Zakarin & Balakay, 2003; Turganbayev & Kazamirchuk, 1999b).

Based on the above objective we can formulate tasks of the project MigRad:

- Develop informational model of the territory of the Semipalatinsk Test Ste on the base of geoinformation technologies and remote sensing data;
- Develop mathematical model of radionuclide migration under the influence of rain flows as the main cause of local redistribution of radioactivity in underlying surface;
- Develop cartographic model of epicenters of wind carry-over of radioactive aerosols taking into account that the main factors of emissive ability of the surface are (i) localization of nu-

- clear tests areas, (ii) distribution of surface activity of radioactive substances and (iii) repeatability of high temperature areas;
- Develop procedure of calculation and analysis of long-range transfer of radioactive aerosol using DERMA model created in the Danish Meteorological Institute (DMI). In the framework of the above-formulated tasks it is necessary:
    1. to create base of digital cartographic information of the STS territory in the framework of geoinformation system,
    2. to create archive of remote sensing data which depicts heat centers on the test site and adjacent areas,
    3. to construct the map of repeatability of heat anomalies over the 10-year period,
    4. to implement the model of radionuclide migration under the action of surface flows and to obtain the maps of redistribution of radioactive contamination over the test site territory,
    5. to develop procedure of mapping of wind soil erosion epicenters on the base of the maps of repeatability of underlying surface overheating, localization of nuclear tests and surface activity of radioactive substances,
    6. to create a package of input parameters for the model DERMA, to carry out simulation of long-range transfer of radioactive substances in the atmosphere and to construct software complex of cartographic analysis of modeling results.

## 2. Object-Oriented Analysis of the Studied Area

GIS-project MigRad was developed in UML (Unified Modeling Language) (*Rambo & Blakha, 2007*) based on object-oriented approach at all stages of project development. Conceptual statements of the approach are presented in the previous section; here we present the design stage based on UML-technology. This stage includes construction of the model of classes and creation of diagrams describing the structure and connections of the system as well as probable scenarios of its usage.

### 2.1. General interaction diagram

Here, the statement of the problem described before will be presented in a form of general interactions diagram (Figure 5). It gives general concept of all technological chain – from database development to modeling of radionuclide migration.

The first step is formation of the database containing historic and remote sensing data. The next stage consists of three parallel processes:

- modeling of surface washing-off of radionuclides;
- construction of the map of localization of explosions with indication of available parameters;
- construction of the map of repeatability of higher temperature on the base of remote sensing data.

The results of modeling of radionuclide migration for the case of rain washing-off are interesting by themselves, and are used as input data of the system. Moreover, they are used for cartographic modeling of epicenters of wind carry-over of radioactive aerosol. The map of epicenters of aerosol carry-over is used further for modeling of long-range transfer of radioactive substances. The main result of GIS-project MigRad is cartographic information on radionuclide transfer and fallout.

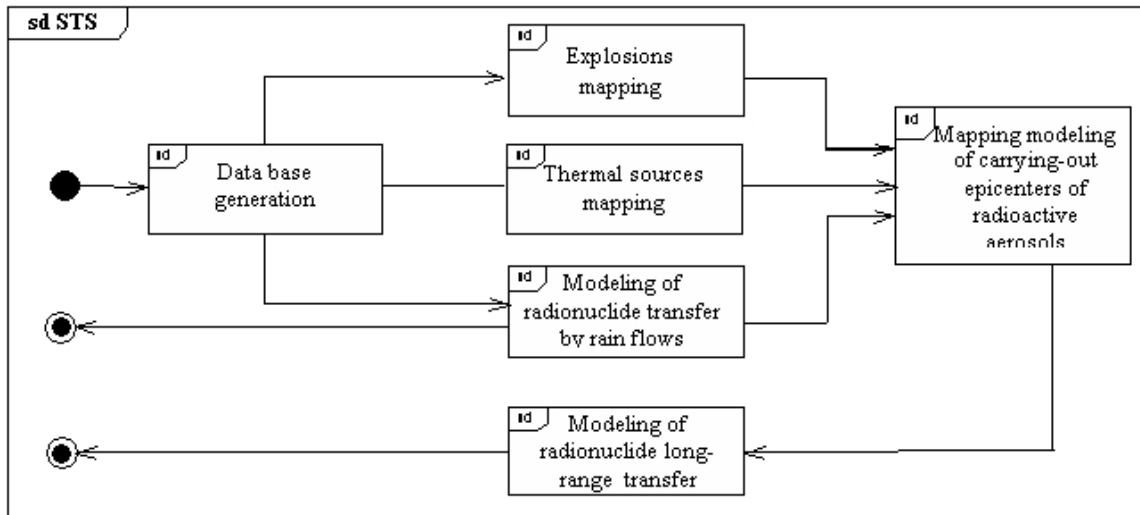


Figure 5. General interaction diagram.

## 2.2. Diagram of classes

Conceptual model gives sufficient amount of information to construct the model of classes. According to the objective of the project we can define the following main classes:

- (i) abstract class “user” and daughter classes “developer” and “customer” (“client”) inheriting its attributes and operations;
- (ii) abstract class “database” and inheriting daughter classes “Cartographic database”, “raster DB” (remote sensing database) and “table DB”;
- (iii) abstract class “model” and its daughter models:
  - surface washing-off of radioactive substances – RUNOFF,
  - mapping of temperature fields according to the remote sensing data – TERMO and
  - long-range transfer of radioactive substances in atmosphere - DERMA;
- abstract class “interface” and daughter classes:
  - “Interface 1” realizing users’ interaction with models,
  - “Interface 2” realizing models’ interaction with databases and
  - (iii) “Interface 3” realizing user’s interaction with databases.

Figure 6 demonstrates the model of classes. This diagram determines attributes and operations of classes as well as relations between them.

## 2.3. Sequence diagram

The general diagram of interactions will be specified using the sequence diagram based on the above-defined classes. In order to avoid overloading of the scheme we will omit the classes of interfaces and draw the main attention to the sequence of actions with non-abstract classes identifying simulating models. The diagram of sequences is a number of “running tracks” which classes “run” exchanging orders and data. Figure 7 shows the sequence of operations applied to solve various problems using MigRad instruments.

At the first stage the procedure of simulation of radionuclides redistribution on the STS territory under the action of surface runoffs is simulated. This procedure includes:

- handling of the user’s application,
- formation of application to the database,
- formation of the package of input information (relief, meteorological data on precipitations, map of initial field of radionuclides, for example, Cs-137, and other data),

- calculation of pollutant transfer with rain runoffs,
- loading of the results of modeling (new fields of Cs-137) into the database.

Practically the same steps are fulfilled

- in calculating thermal fields and their statistical processing with calculation of the map of repeatability of high temperatures
- in determining the epicenters of carry-over of radioactive aerosol by winds,
- in calculating long-range atmospheric transfer of radionuclides.

Certainly, the above stages have different input parameters (some of them are the results of calculations of the previous stages), models and output results. All these factors are taken into account in specification of UML-diagrams.

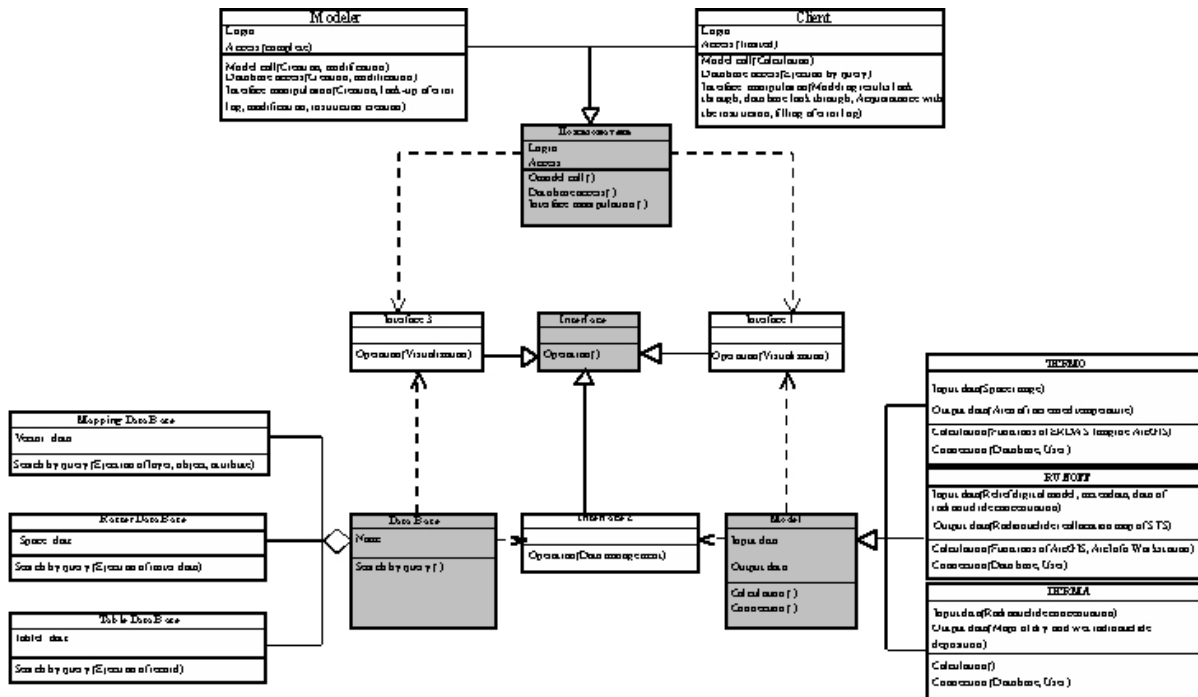


Figure 6. Classes diagram with connections.

## 2.4. Database structure

As it was noted above the class “Database” aggregates three databases “Map DB”, “Raster DB” and “Table DB”.

Map data for the test site and adjacent areas include the following information (*Turganbayev & Kazamirchuk, 1999a; Zakarin & Balakay, 2002*):

- topographic map of the Semipalatinsk test site and its surrounding areas;
- soil map of the test site territory;
- information on nuclear explosions as a map where dots identify the places of explosions, and
- geological map of the test site territory with identification of stratigraphic subdivisions, magmatic complexes, tectonic disruptions and mineral resources;
- geological map of the Balapan testing site;
- data on hydrogeology of the test site;
- map of chemical composition and general mineralization of fracture waters on the Balapan testing site;
- data on hydrogeology of the Semipalatinsk test site;
- watershed map of the STS territory;

- map of samples and measurements (alpha, beta, MED (h=3cm), MED (h=1m), Cs-137, Sr-90).
- Point data by the results of automatic gamma-spectrometric survey for five radiation traces (Co, Cs, Ka, OK);
- Integrated contamination by radionuclides ( $\alpha$ ,  $\beta$ ,  $\gamma$  - radiation);
- Map of aerial gamma-spectrometric survey of contamination of the test site territory by cesium-137 ( $\text{Ci}/\text{m}^2$ );
- Map of the results of aerial gamma-spectrometric survey of “Jubileynoye”;
- Map of the results of aerial gamma-spectrometric survey of the exposure rate ( $\mu\text{R}/\text{hour}$ );
- Map of test site contamination with plutonium-239 ( $\text{Bq}/\text{kg}$ );
- Map of exposure rate ( $\mu\text{R}/\text{hour}$ );
- Map of radioactive traces formed after over ground explosions.

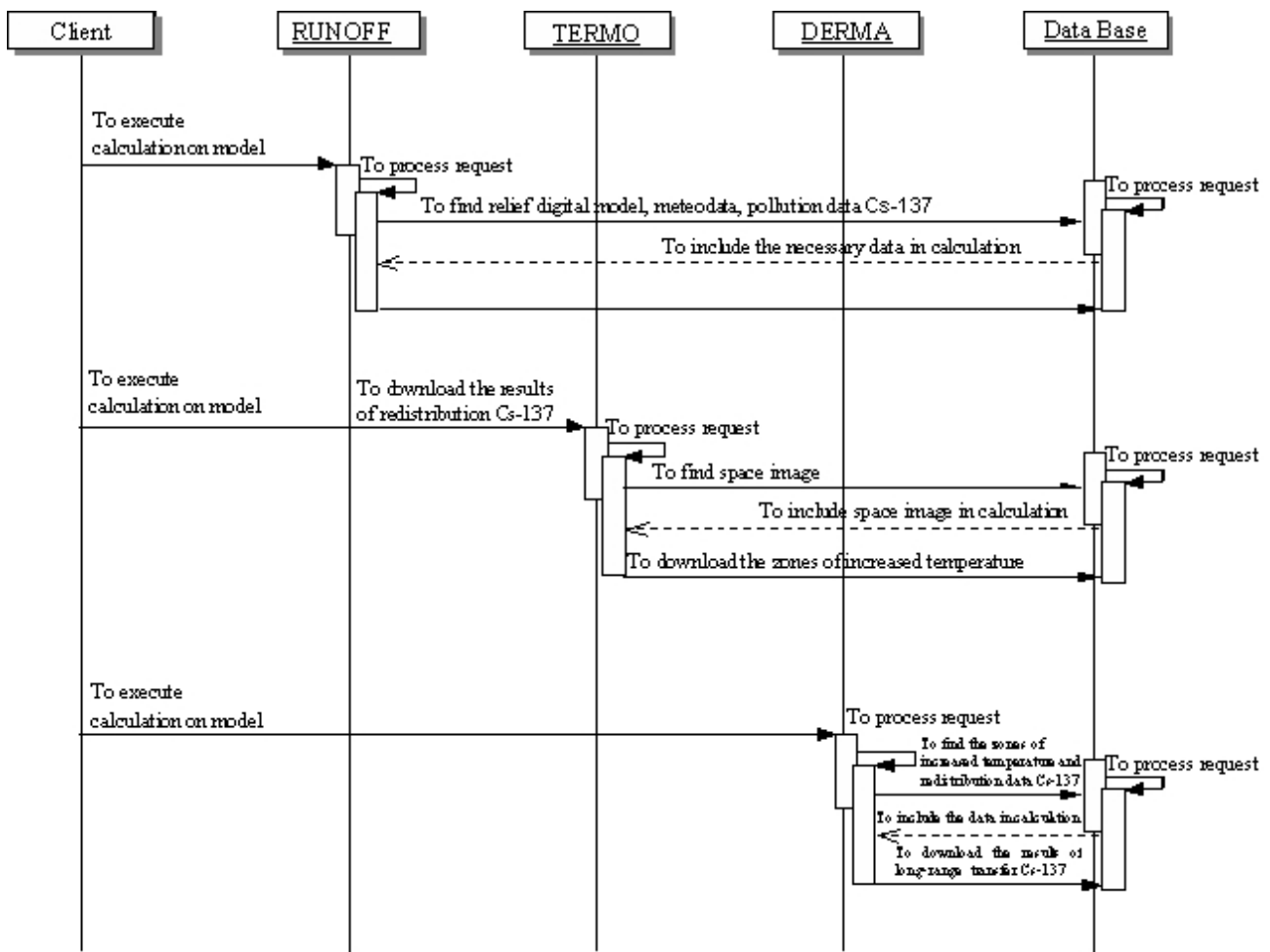


Figure 7. Sequence diagram of MigRad project.

The above-listed data as digital maps in format of ArcGIS database are included in GIS-project MigRad. This format is a state-of-the-art presentation of spatially-distributed data, applied logics and instruments for their control.

The remote sensing data for the test site are presented in the corresponding database as AVHRR/NOAA and MODIS/Terra satellite-based images for the 10-year period, from 1997 to 2007, and are designated for statistical analysis of thermal anomalies in TERMO procedure.

“Table BD” contains xls-tables with information about all explosions made on the test site territory (Bocharov *et al.*, 1989), data on precipitations for the warm period of the year for 13 weather stations, results of aerial gamma-spectrometric survey for thorium, uranium, potassium and other

historic data.

Moreover, corresponding databases are also used for storage and analysis of the results of mathematical and cartographic modeling and technical processing of satellite-based images. The user may analyze these results getting direct access to required databases through corresponding interfaces.

Presented UML-diagrams and description of the database give general idea of the structure and functions of GIS-project MigRad. We will consider the models making conceptual part of GIS-project in more detail.

### 3. Modeling of Radionuclides Migration with Surface Waters

Horizontal redistribution of radionuclides over the territory occurs under the action of a great number of factors. The most important of them is washing-off of the upper soil layers by surface waters, which causes migration of accumulated in them radioactive substances (*Zakarin & Balakay, 2003b; Balakay, 2003*). Such processes are accompanied by formation of new zones of radionuclide accumulation in the areas of relief lowering, which dramatically change spatial structure of dose status of population (*Zakarin et al., 2003*). This section considers the main methods used to calculate water soil erosion and describes model RUNOFF realized in the framework of GIS-project MIGRAD.

#### 3.1. RUNOFF Model: basics and equations

Redistribution of radioactive substances under the action of surface water flows caused by rain or snow melting is directly connected with washing-off and accumulation of the soil cover particles.

Most of contemporary methods applied to calculate water erosion use various forms of universal erosion equation (USLE) developed in the USA (*Wischmeier & Smith, 1978; Foster, 1979*).

The universal erosion equation was used in developing of a large number of models which use the same influencing washing-off factors but modernized calculation formulas, in particular, these are models RUSLE, EPIC, MUSLE (*Kuznetsov & Glazunov, 1996*). One of the first to suggest such model was G.I. Shvebs (*Shvebs, 1974; 1981*), who called it logical-mathematical model. It is based on the dependence between the runoff turbidity, strength of precipitations and intensity of water yield.

There is also a hydro mechanical model (*Zvonkov, 1963; Mirtzhulava, 1970; 1976; Kuznetsov, 1973*) in which the flow bed is schematically presented by uniform globe-shaped components (units) connected with each other by coupling forces. In this approach washing-off in any section line may be expressed as weight of components torn away per unit of time.

It is also necessary to mention the equations for calculating soil and ground washing-off developed by (*Mirtzhulava, 1970; 1976*), which are the most popular equations with Russian scientists. The model is based on the experimental-theoretical equation of soil and ground washing-off, whose main argument is ratio of the speed of water motion down the slope to the critical flux speed, above which washing out of soil starts.

An analysis of the above-listed models showed that the most suitable model for the test site conditions (in terms of availability of input information) is the equation of water erosion suggested in (*Haith et al., 1984*). This erosion model enables to take into account real distribution of precipitations during warm seasons of the year, and calculations of washing-off are carried out for every rain at the moment of time  $t$  by the formula:

$$\bar{X}_t = 21 \cdot A^{0.12} \cdot Q_t^{1.12} \cdot \left( \frac{\frac{R_t}{D_t}}{R_t - 0.2 \cdot W_t} \right)^{0.56} \cdot K \cdot L \cdot S \cdot P \cdot C_t \quad (2.1)$$

Here  $X_t$  is washing-off of soil from a unit area per year (washing-off module) (t/hectare),  $A$  is the slope area (hectares);  $Q_t$  is the thickness of water flow (cm);  $R_t$  is the amount of precipitations (cm),  $D_t$  is duration of precipitations (hour);  $K$  – erodibility factor (soil washing-off),  $L$  – factor of slope length,  $S$  – factor of slope angle,  $P$  – factor of erosion-preventive measures,  $C_t$  – economic-agricultural factor.

$C_t$  is determined from the equation:

$$C_t = 1 - CP_t, \quad (2.2)$$

where  $CP_t$  is the fraction of slope covered with vegetation which can be estimated by the data of topographic maps or results of remote sensing. For the territory of the Semipalatinsk Test Site factor  $P$  may be neglected and taken equal to 1, as no erosion-preventive measures are taken on the territory of the Test Site.

The thickness of surface flows (cm) is calculated by the formula:

$$Q_t = \frac{(R_t - 0.2 \cdot W_t)^2}{R_t + 0.8 \cdot W_t} \quad (2.3)$$

Parameter  $W_t$  (cm) is determined from the relation:

$$W_t = \frac{2540}{CN_t} - 25.4, \quad (2.4)$$

where  $CN_t$  is soil parameter which describes relation between the amount of precipitations and thickness of surface flows and depends on soil moisture.  $CN_t$  is determined using the techniques suggested in (*Ograsky & Mockus*).  $W_t$  characterizes amount of water permeated into soil on a given slope.

The factor of length  $L$  is determined from the relation:

$$L = \left[ \frac{l}{22.1} \right]^p, \quad (2.5)$$

where  $l$  is the slope length, m;  $p$  is the exponent for length equal to 0.2, 0.3, 0.4 and 0.5, respectively, for slopes ( $\alpha$ ) < 1, 1 - 2, 3 - 5 and >5 %. The slope factor  $S$  is determined from the relation:

$$S = 0.065 + 4.56 \sin \alpha + 65.41 \sin^2 \alpha. \quad (2.6)$$

The values of erosion potential of precipitations are obtained by statistical treatment of rather long time series. According to the data presented in (*Tarabrin, 1976; Larionov, 1993*) for the territory of Semipalatinsk oblast  $R$  is approximately equal to 3 units of erosion potential of precipitations (EPP). The factor of soil washing-off  $K$  was determined according to the method suggested in references (*Tarabrin, 1976; Wischmeier & Mannering, 1969; Schwertman et al., 1990*).

Surface redistribution of radionuclides was calculated on the base of results of modeling of soil washing-off  $X_t$  and initial field of surface activity of radioactive substances  $C_0$ . The most complete data obtained by aerial gamma-spectrometric survey of the test site territory refer to Cs-137, and therefore this substance was chosen for further calculations. Redistribution of Cs-137 was calcu-

lated by the formula:

$$C_t = \frac{X_t}{\rho_s h_s} C_0, \quad (2.7)$$

where  $C_0$  and  $C_t$  are surface activities of Cs-137 ( $\text{Ci}/\text{m}^2$ ) before and after washing-off by rain runoffs,  $\rho_s$  is soil density and  $h_s$  is thickness of soil layer (m), whose radiation forms surface activity of Cs-137.

It should be noted that suggested model RUNOFF refers to the class of models with lumped parameters. As studied processes are surface distributed processes, calculations were made for each cell of the grid, and all intermediate and final results are obtained as grid-maps.

In constructing the accumulation map we took into account cross-flows between the cells. As initial data for them we used grid-maps of rain washing-off of radionuclides.

### 3.2. Structure of model and data flow

As it is seen from the foregoing, RUNOFF model unites both calculation formulas and data array. Therefore the model whose structure is presented on the scheme (Figure 8) consists of two stages – data preparation (vertical chain of procedures) and accurate calculation (horizontal line).

Data preparation includes the following operations:

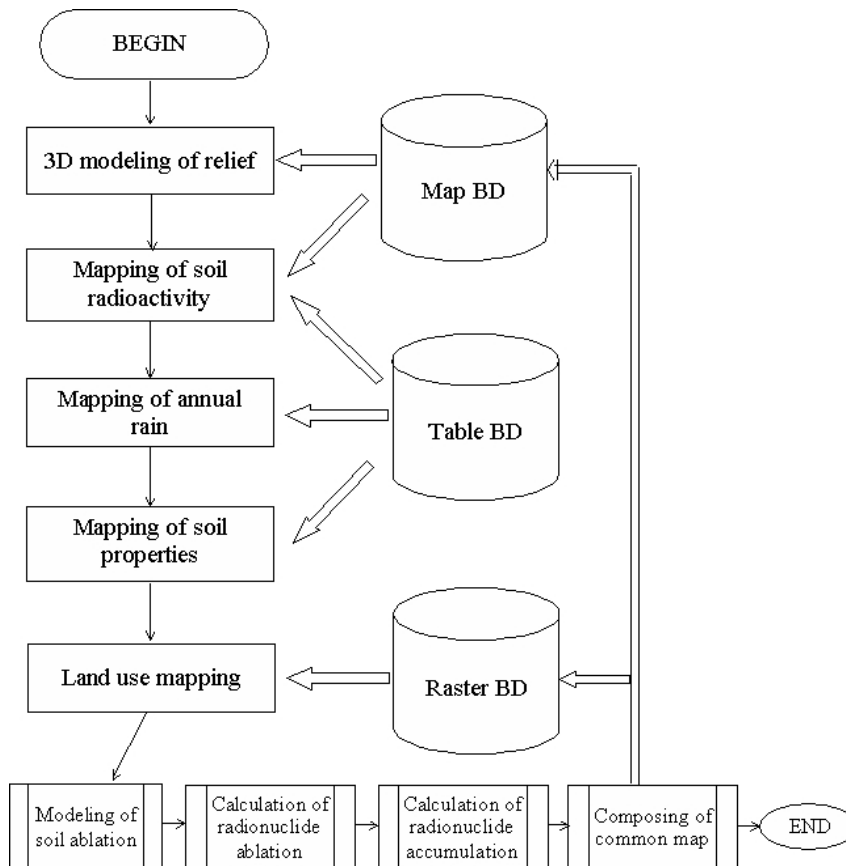


Figure 8. The structure of the RUNOFF model.

- Construction of hypsometry of calculated test site. This task was solved by digitizing of topographic maps of scale 1:200000 and creating of digital relief model in ArcGIS (Turganbayev et al., 1999). The results of this procedure are shown in Figure 9.

- Construction of grid-map of surface activity of radionuclide  $C_0$  on the base of the data of aerial gamma-spectrometric survey of test site contamination by Cs-137 ( $Ci/m^2$ ) (survey dated by 1994). The map of surface soil activity is shown in Figure .
- Construction of grid-map of average annual amount of precipitations by the data of 13 weather stations located around the test site. The data on the amount of snow and rain used in calculations correspond to the average annual data for many-year period of observations (*Climate USSR, 1967*). Duration of precipitations was chosen such as to provide rain intensity equal to 0.5 mm/hour. Thus, calculations were made for average annual precipitations on the test site territory assuming that monthly amount of precipitations fall during one rain. Figure 10 shows spatial distribution of total annual amount of precipitations (*Akhmetzhanov & Kazamirchuk, 2000*).
- Calculation and mapping of underlying surface properties – erosion and water permeability (using technique developed by Ograsky and Mockus). Figure 11 shows maps of soil parameters for the test site territory.
- Calculation and mapping of economic – agricultural factor. Figure 12 illustrates this process – using Terra/MODIS images NDVI matrix is constructed and then using formula (2.2) mapping of economic – agricultural factor is made.

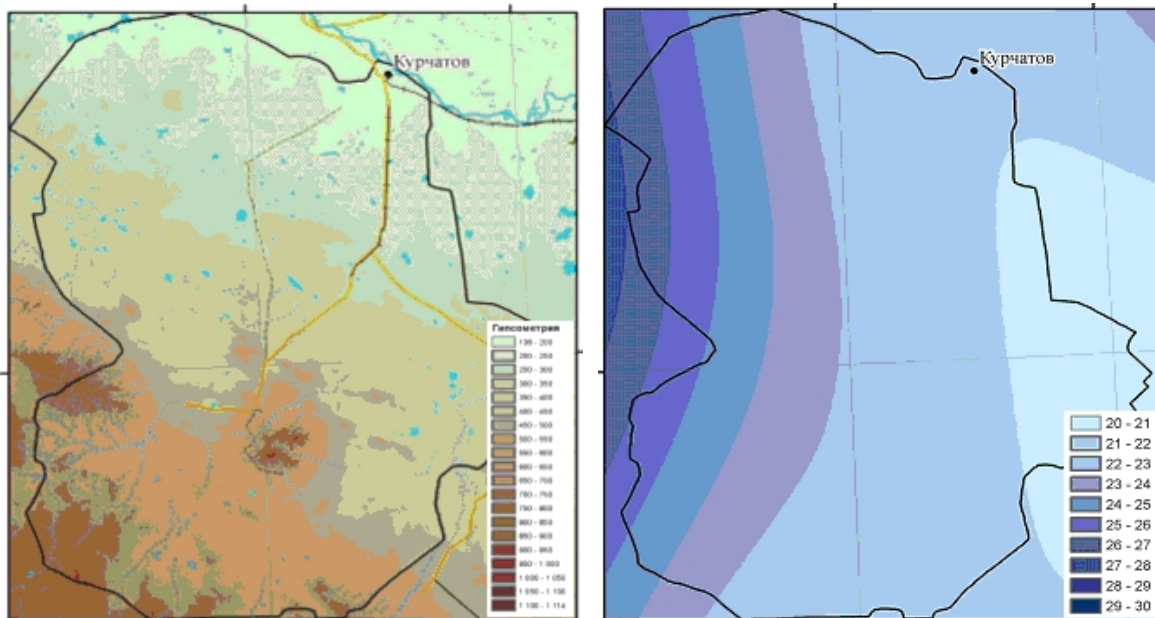
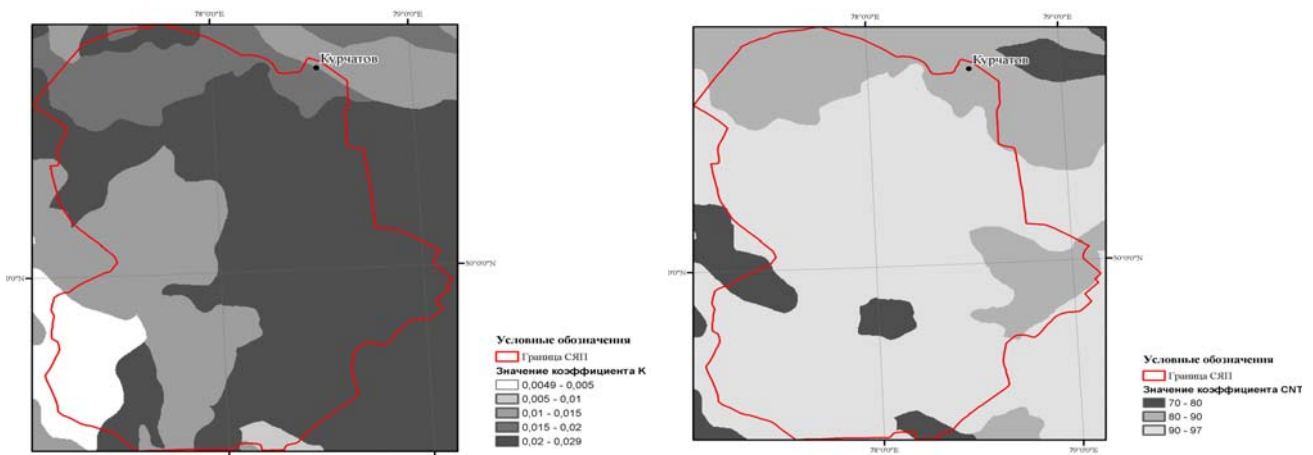


Figure 9. Digital model of STS relief. Figure 10. Map of spatial distribution of annual precipitations (cm)



Map of spatial distribution of soil erosion coefficient value

Map of spatial distribution of water permeability coefficient value

Figure 11. Maps of soil parameters  $K$  and  $CN_i$

### 3.3. Modeling results

The results of calculation of annual water erosion made on the base of average annual data for precipitations are presented in Figure 14. Average washing-off intensity was 3.4 t/ hectare, which is a permissible soil loss according to American classification (*Derbentsova, 2006*). Making the map of washing-off intensity per year (Figure 14) we used the following classification (*Derbentsova, 2006*): insignificant washing-off – 0.5 t/hectare; little washing-off – 0.5 – 1 t/ hectare; intermediate washing-off – 1 – 5 t/ hectare; strong washing-off – 5 – 10 t/ hectare; very strong – more than 10 t/ hectare.

The highest values of washing-off are observed for small sections in mountainous areas: mountains Delegen, Naimanzhal, Maramyk, Saragozhal and Zhangyztau. Minimal values are observed on the flat part of studied territory. The thickness of washed-off soil ranges from 0 to 5 cm, and the thickness of accumulated soil varies from 0 to 2 cm (Figure 15).



**Figure 12.** Stages of construction of the map of economic – agricultural factor.

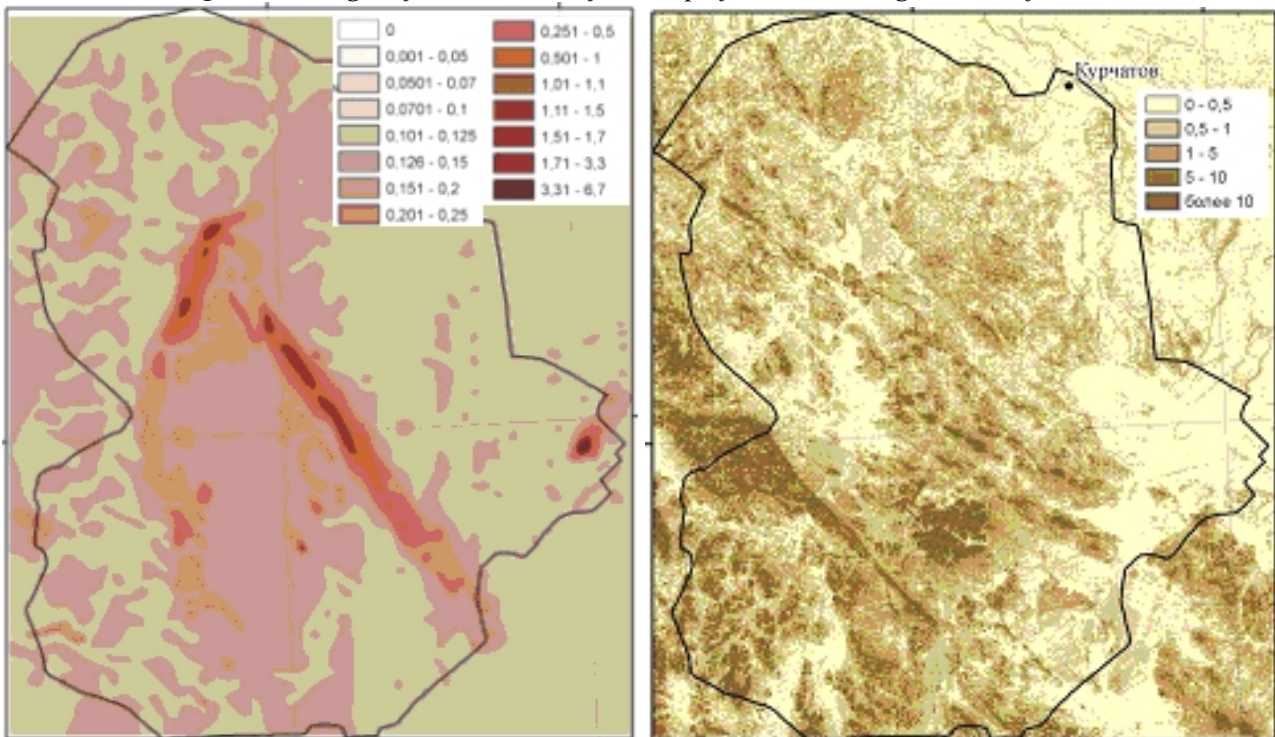


**Figure 13.** Map of spatial distribution of surface soil activity ( $C_i/m^2$ ). **Figure 14.** Map of surface washing-off (t/hectare).

activity. As initial data we used the data of the 1994 aerial gamma-spectrometric survey and studied migration of radionuclides for 12 years up to the year 2006. Figure 16 illustrates computer-simulated results of redistribution of radionuclides under the action of surface flows. It is seen from the figure that the value of surface activity decreased in the mountainous areas and increased in the accumulation areas (streams, ravines, riverbeds) (Zakarin & Balakay, 2003ab; Balakay, 2003; 2001). Maximal value equal to  $8.9 \text{ Ci/m}^2$  was observed near Naimanzhal mountains. The difference in values of Cs-137 surface activity in 1994 and 2006 is shown in Figure 17, in which blue color (left picture) corresponds to decrease in activity values in 2006 and red color (right picture) depicts activity increase.

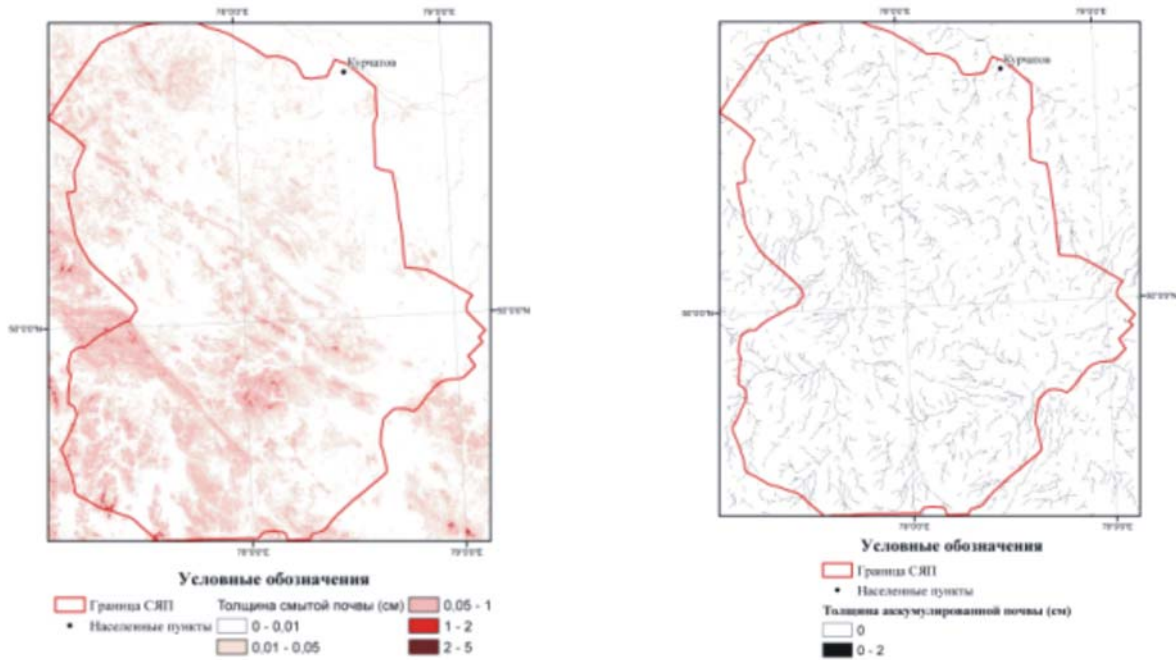


**Figure 15.** Spatial distribution of runoff and accumulated soil (left) - The thickness of washed-off soil (cm), and (right) The thickness of accumulated soil (cm).

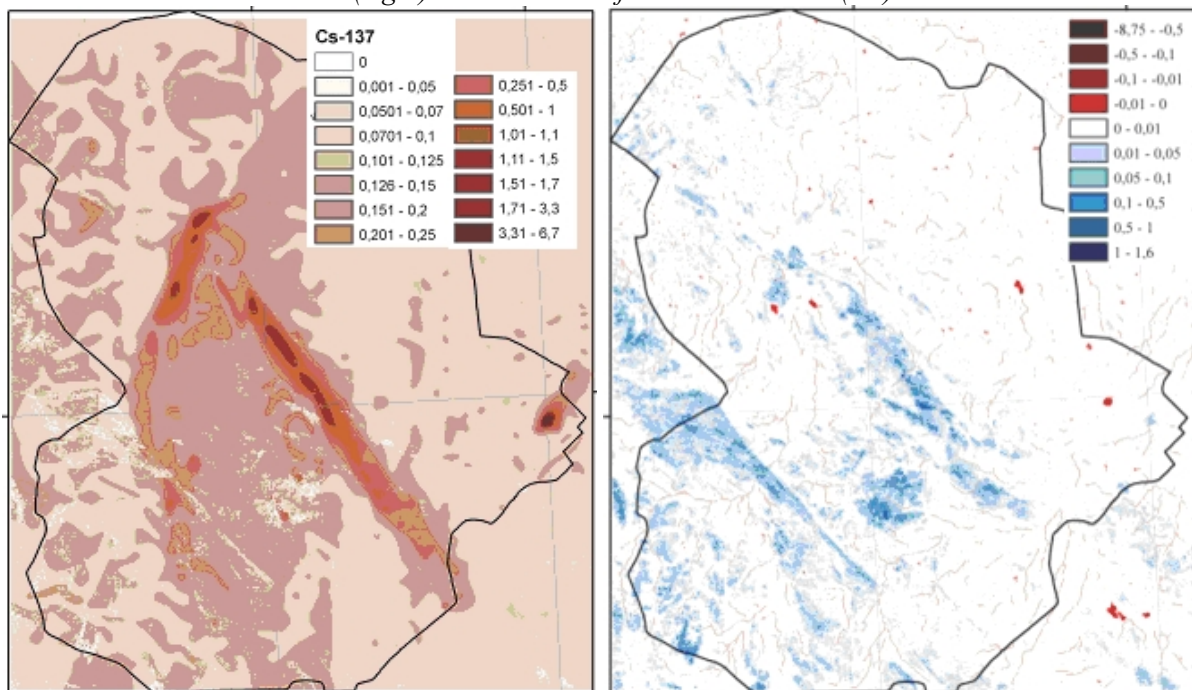


**Figure 16.** Cs-137 surface activity in 2006. ( $\text{Ci/m}^2$ ). **Figure 17.** Difference in values of Cs-137 surface activity before and after 12-year summer rain runoff.

## 4. Mapping of High Temperature Zones on the Territory of Semipalatinsk Test Site

According to the problem statement in order to determine sources of radioactive aerosol it is necessary to carry out statistical treatment of remote sensing data in thermal channel and to determine places of permanent overheating of the surface. For this purpose was developed model TERMO oriented on processing of AVHRR/NOAA and MODIS/Terra archive data.

At the stage of processing of raster images model TERMO is realized as a graphical model with the usage of the set of instrumental tools of so-called the ERDAS IMAGINE program complex (ERDAS, 1999). The graphical model (Figure 18 *Figure* ) is a block-diagram consisting of the following functions and operators of ERDAS IMAGINE package:

- INPUT RASTER – input image of the test site in \*.img format and geographical adjustment UTM zone 43/WGS 84.
- SUBSETTING – instrument for cutting out of a part of the photograph. It enables to diminish the image and to include into studying only area of interest (AOI).
- CONVOLUTION (LOW PASS) – function of image averaging. Operation of convolution makes averaging of parameter value in each pixel with respect to the values of surrounding pixels. This model uses convolution of the size of a pixel window.
- CLASSIFICATION – function of image subdividing into classes. This operation is used to discover classes corresponding to the given temperature interval.
- VECTORISATION – function of transfer of raster image into vector image or map. As a result of operation Polygon map with temperature isolines is constructed.
- OUTPUT VECTOR – output thematic layers of test Polygon.

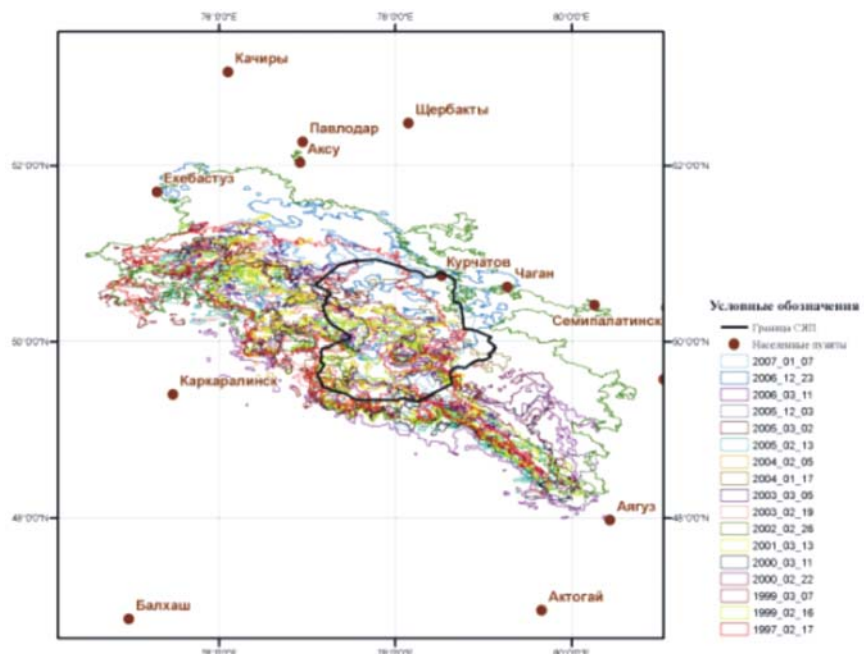
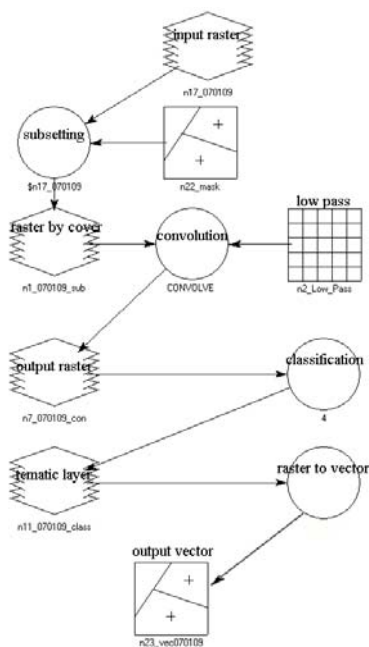


**Figure 18.** Block-diagram TERMO. **Figure 19.** Map of outlines of high temperature zone constructed on the base of remote sensing data for the 1997 – 2007 period.

According to the data of such processing the map of outlines of high temperature zones for the 10-year period, from 1997 to 2007, was constructed (Figure 19 *Figure* ).

At the stage of statistical treatment of vector data in TERMO model operations of ArcGIS package are used. This package fulfills the following operations:

- Filtration of small polygons related to small and unrepeatd heat centers;

- Construction of a binary grid as a mask with “0” elements corresponding to zero overheating and “1” corresponding to high temperature;
- Calculation of repeatability of thermal anomaly by summation of masks;
- Construction of the resulting map with gradation “low repeatability” – 0-30%, “average repeatability” – 30-70%, “high repeatability” – 70-100%.

The resulting map of repeatability of high temperature zones is presented in Figure 20. The right side of the figure shows the map corresponding to maximal repeatability of high temperature zones. The figure shows that on the Polygon territory such zones are located around testing sites Delegen and Experimental field, where a great number of nuclear explosions were made. Moreover, one can make a conclusion that numerous nuclear tests activated the fracture passing through the Polygon territory and it, probably, became the sources of heat.

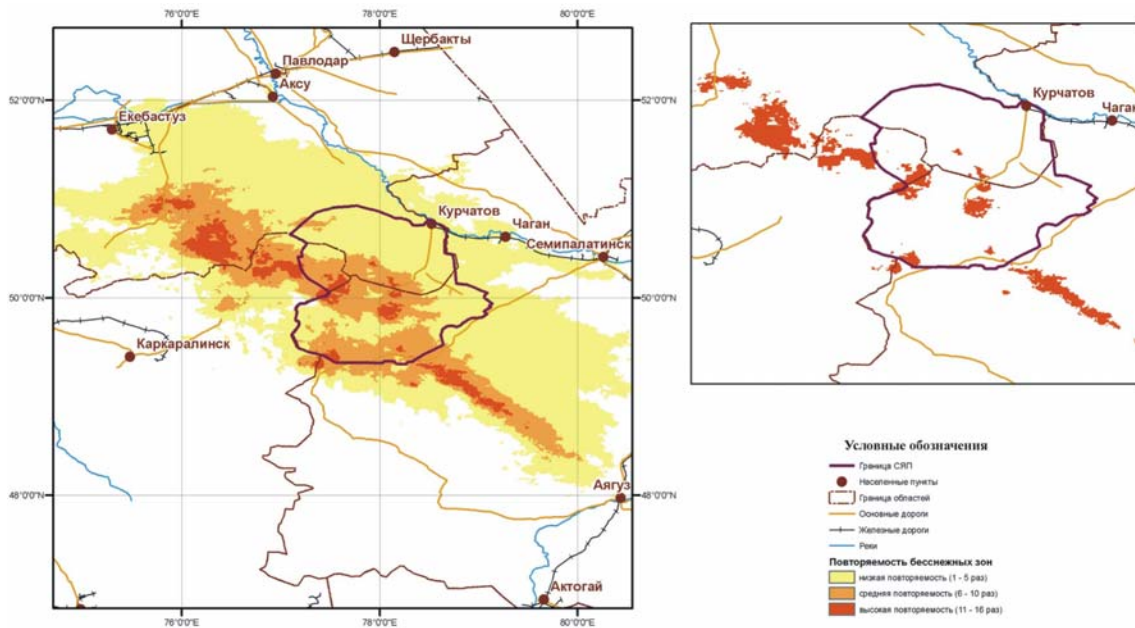


Figure 20. Map of repeatability of high temperature zones.

## 5. Mapping of Epicenters of Radioactive Aerosol Transport

The procedure of detecting places of maximal probable localization of sources of wind carrying out of aerosols was developed in accordance with the problem statement. The method is based on the assumption that under other equal conditions (vegetation cover, types of soil cover, etc.) the defining factors are the following three factors:

- Places of localization of testing explosions of nuclear devices,
- Distribution of surface activity of radionuclide (here Cs-137) calculated for the moment of modeling (for the year 2006),
- Repeatability of high temperature zones increasing erosion ability of underlying surface.

Vector maps corresponding to the above-listed factors were transformed into grid-format and then on the base of combination function (**OR** and **AND**) the map of localization of sources atmospheric radiation pollution was made. Figure 21 illustrates this procedure. The results of such analysis showed that the sources of carrying out of radioactive substances are three areas situated on the testing grounds Experimental Field, Degelen and Balapan. High radiation contamination of the areas of localization of underground nuclear tests (Delegen and Balapan) is confirmed by the data of (Strilchuk *et al.*, 2005). The experimental field is also a source of radiation hazard as many surface nuclear explosions were made there.

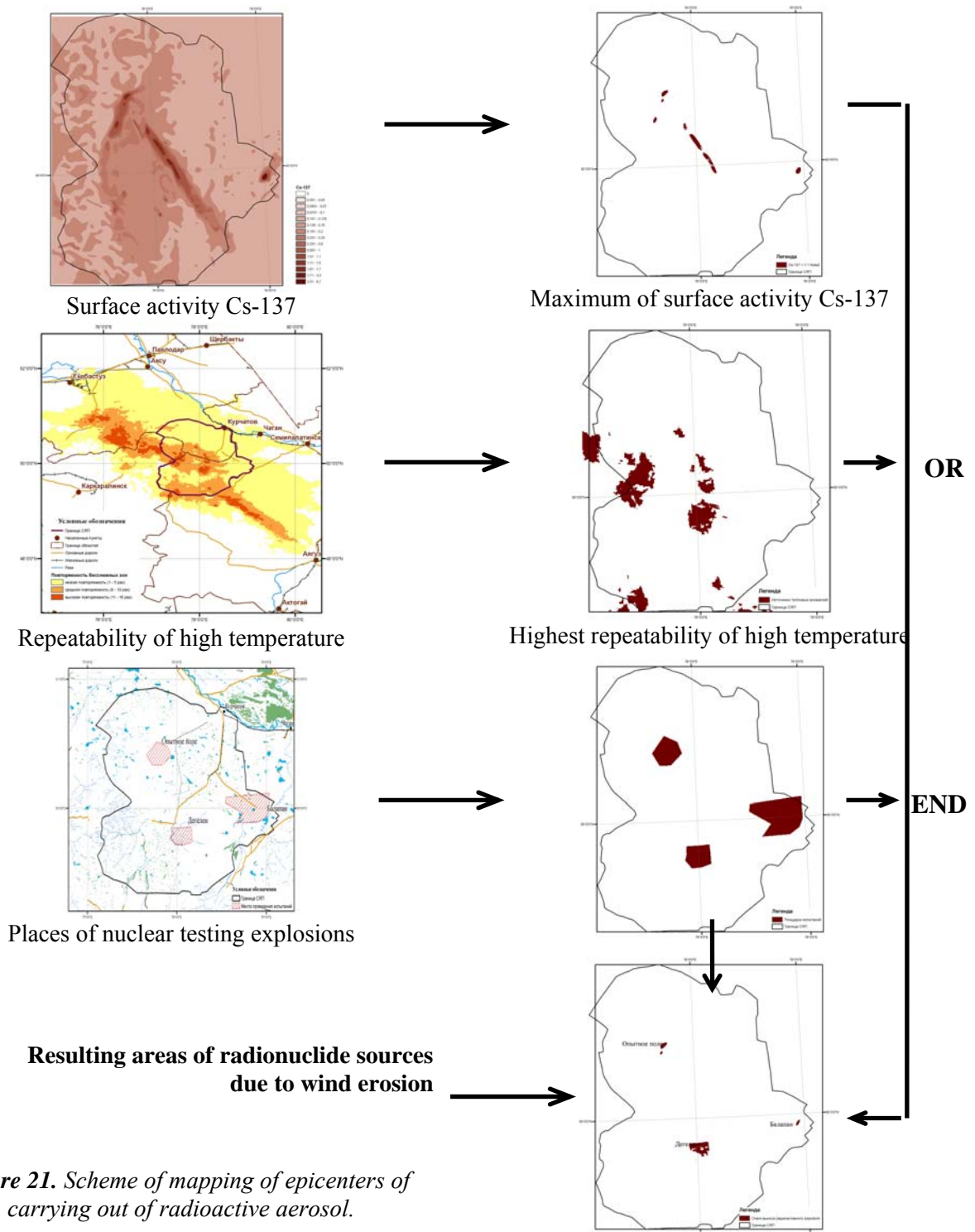


Figure 21. Scheme of mapping of epicenters of carrying out of radioactive aerosol.

## 6. Transboundary Atmospheric Transport of Radioactive Substances

The most complicated function of MigRad system is calculation and analysis of long-range (transboundary) transport of radionuclides from the test site territory. The module for calculations is based on DERMA model (see the next section) and consists of three stages:

- Formation of the input data package for model DERMA,
- Calculations using model DERMA,
- Treatment of the modeling results using specially developed procedure.

The problem of long-range transport of pollution substances in atmosphere refers to the class of very sophisticated problems as it is necessary to take into account great number of processes such as advection, turbulent diffusion, dry and wet precipitation and many other factors. As a rule, such models are developed by large groups of specialists with usage of the latest and most powerful computer equipment. By the present time a series of such models (*Schopp et al., 1999; Ishikawa, 1995; Vinogradova & Yegorov, 1996; Galperin et al., 1995; Baklanov et al., 2006*) which are used in European, American Asian computer centers.

Special attention is paid to modeling of long-term transport of polluting substances. This direction started to develop at a rapid pace after the accident at Chernobyl nuclear power plant in 1986. Models calculating the impact of the accident on European countries were developed (*Klug et al., 1992; Lauritzen & Mikkelsen, 1999*).

Comparison of 50 models in the European Tracer Experiment (ETEX) showed that model DERMA (the Danish Emergency Response Model for Atmosphere) gave one of the best results (*Van Dop et al., 1998*). Therefore to model long-range transport of radioactive substances from the STS test site we chose this model. DERMA was developed by Danish Meteorological Institute (DMI) and it is a 3D Lagrangian-type numerical model (see 6.1), and can be used for modeling of atmospheric transport, dispersion, precipitation and decay of radioactive substances (*Baklanov et al., 2006; Mahura et al., 2005*). Model DERMA was run on the supercomputer NEC SX6. As meteorological data this model used numerical weather prognoses (NWP) obtained as a result of calculations of model HIRLAM (High Resolution Limited Area Model) functioning in DMI or as prognosis data of global model of the European Center for Medium-Range Weather Forecasts (ECMWF).

## 6.1. DERMA Model: basics and equations

The **D**anish **E**mergency **R**esponse **M**odel for **A**tmosphere (**DERMA**) is a numerical three-dimensional atmospheric dispersion model of Lagrangian type. This model describes atmospheric transport, diffusion, deposition, and radioactive decay within a range from about 20 kilometers to the global scale. DERMA is developed at the **D**anish **M**eteorological **I**nstitute (**DMI**) for nuclear emergency preparedness purposes and integrated with the ARGOS system. This model uses **N**umerical **W**eather **P**rediction (**NWP**) model data from different operational versions of the **H**igh **R**esolution **L**imited **A**rea **M**odel (**HIRLAM**) running at DMI or from the global model of the European Center for Medium-Range Weather Forecast (ECMWF). The DERMA model structure and its dispersion modelling block were described by *Sørensen (1998)* and *Sørensen et al. (1998)*, and the deposition modelling block – by *Baklanov & Sørensen (2001)*.

Earlier comparisons of simulations by the DERMA model vs. the ETEX experiment involving passive tracers showed very good results. Institutions (in total 28) from the European countries, USA, Canada, and Japan contributed to the real-time model evaluation. Based on analyses from this experiment, the DERMA model was emphasized as being very successful (*Graziani et al., 1998*). In order to verify the deposition parameterizations and study effects of deposition, DERMA simulations for several cases – (the INEX and RTMOD exercises, and Algeciras accidental <sup>137</sup>Cs release in Spain) – were conducted taking into account different approaches for the deposition processes. In particular, the comparison of simulation results for the Algeciras accidental release with measurement data from the European monitoring network were analyzed by *Baklanov (1999)* and *Baklanov & Sørensen (2001)*.

The basic equation for concentration of radioactive species in the atmosphere,  $c$ , taking into account the removal processes in the atmosphere and the interaction of the radionuclides with the Earth's surface, can be expressed:

$$\frac{\partial c}{\partial t} = -\text{div}(\mathbf{u}c) + \text{Turb} - D\text{dep} - W\text{dep} - \lambda c + \lambda'c' + \text{Res} + Q, \quad (1)$$

where:

- $div(\mathbf{u} c)$  - advection transport by vector velocity  $\mathbf{u}$ ,
- $Turb$  - turbulent diffusion of passive tracers in the atmosphere,
- $Ddep$  - dry deposition on the surface,
- $Wdep$  - wet deposition processes,
- $\lambda c$  - radioactive decay to daughter nuclides,
- $\lambda'c'$  - decay from parent nuclides,
- $\lambda$  - decay constant for the corresponding nuclide,
- $Res$  - resuspension processes,
- $Q$  - release source.

For nuclear emergency response and post-accidental analysis, several versions of the DERMA model including different approaches and complexity of parameterizations of the deposition processes can be used. Let us describe the version of the DERMA model which was selected for the long-term simulation of contamination.

The temporal resolution of the currently available operational NWP model data is one or more hours. The DERMA model interpolates these data linearly in time to the advection time steps. The advection time step of DERMA is equal to e.g. 15 minutes (which is a typical turn-over time of the large vertical eddies within the boundary layer of the atmosphere). Thus, we assume that material released into the boundary layer becomes well mixed in this layer within a few time steps. Moreover, the assumption of complete mixing within the boundary layer is used in the DERMA model. In order to simulate a cold release at ground level, and following the assumption of complete mixing, all particles are emitted at equidistant heights from the surface to the top of the boundary layer. These particles are advected by the three-dimensional wind fields from the NWP model.

### **Turbulent Diffusion and Transport**

DERMA is a dispersion model based on a multi-level puff parameterization (Sørensen & Rasmussen, 1995; Sørensen, 1997). A “puff” (i.e. a concentration field surrounding a particle) is associated with each particle adding up to the total concentration field. In the horizontal, a Gaussian distribution of the concentration is assumed for each puff. For puffs inside the boundary layer, an assumption of complete mixing is employed in the vertical, while for puffs above the boundary layer, a Gaussian distribution is employed.

For a puff  $p$  positioned at point  $(x_p, y_p, z_p)$  above the boundary layer ( $z_p > h$ ), the Gaussian formula given by Zannetti (1990) is used. The height of the boundary layer (the mixing layer) is denoted  $h$ . The puff contributes to the concentration field at the spatial location  $(x, y, z)$  with the amount  $C_p$ :

$$C_p = \frac{Q_p}{(2\pi)^{3/2} \sigma_y^2 \sigma_z} \exp \left\{ -\frac{1}{2} \left( \frac{x - x_p}{\sigma_y} \right)^2 - \frac{1}{2} \left( \frac{y - y_p}{\sigma_y} \right)^2 \right\} \times \left( \exp \left\{ -\frac{1}{2} \left( \frac{z - z_p}{\sigma_z} \right)^2 \right\} + \exp \left\{ -\frac{1}{2} \left( \frac{z + z_p}{\sigma_z} \right)^2 \right\} \right), \quad (2)$$

where:

- $C_p$  – amount (mass) of tracer gas associated with the puff depending on the emission rate,
- $\sigma_y, \sigma_z$  - horizontal and vertical standard deviations of the spatial concentration distribution.

For a puff located within the boundary layer (i.e. for  $z_p \leq h$ ), we assume complete mixing in this layer, and therefore the following expression for the contribution to the total concentration field is used:

$$C_p = \frac{Q_p}{2\pi\sigma_y^2 h} \exp\left\{-\frac{1}{2}\left(\frac{x-x_p}{\sigma_y}\right)^2 - \frac{1}{2}\left(\frac{y-y_p}{\sigma_y}\right)^2\right\} \delta(z, h), \quad (3)$$

$$\delta(z, h) = \begin{cases} 1 & \text{for } z \leq h, \\ 0 & \text{for } z > h. \end{cases} \quad (4)$$

From Gifford's random-force theory (Gifford, 1984) the following expression for the horizontal standard deviation is obtained:

$$\sigma_y^2 = 2K_y t_L \left\{ \tau - (1 - e^{-\tau}) - \frac{1}{2}(1 - e^{-\tau})^2 \right\}. \quad (5)$$

The parameter  $\tau$  is the travel time,  $t$ , in units of the Lagrangian time scale,  $t_L$ , ( $\tau = t/t_L$ ). For the simulations, we have used the value of the horizontal eddy diffusivity,  $K_y$  of  $6 \cdot 10^3 \text{ m}^2/\text{s}$ , and for the Lagrangian time scale,  $t_L$ ,  $10^4 \text{ s}$ .

The expression above has the following asymptotic expressions:

$$\sigma_y^2 = \begin{cases} \frac{2}{3} K_y t_L^{-2} t^{-3} & \text{for } t \ll t_L, \\ 2K_y t & \text{for } t \gg t_L. \end{cases} \quad (6)$$

The short-time asymptotic expression is derived also by Smith (1968) by assuming an exponential auto-correlation using the conditioned particle motion theory. The large-time asymptotic behavior is the well known Fickian diffusion expression, which is also the limit of Taylor's statistical theory of diffusion.

The selected value of  $K_y$  for the horizontal eddy diffusivity was obtained by fitting results of DERMA using DMI-HIRLAM data to the official set of the ETEX tracer gas measurements (Sørensen, 1998). The horizontal and temporal resolutions of NWP data define an upper limit of the value of the horizontal eddy diffusivity mainly describing sub-grid scale diffusion.

For puff centers above the boundary layer, a Gaussian distribution is assumed for the vertical spatial distribution using the following expression for the standard deviation,  $\sigma_z$ :

$$\sigma_z^2 = 2K_z t_L \left\{ \tau - (1 - e^{-\tau}) - \frac{1}{2}(1 - e^{-\tau})^2 \right\} = \left( \frac{K_z}{K_y} \right) \sigma_y^2. \quad (7)$$

The height of the boundary layer is estimated by a bulk Richardson number approach (Sørensen et al., 1996). This approach is useful in cases where the vertical resolution of temperature and wind is limited as e.g. in output from NWP models. The bulk Richardson number,  $Ri_B$ , at height  $z$  above the ground surface is given by the following expression:

$$Ri_B = \frac{gz(\theta_v - \theta_s)}{\theta_s(u^2 + v^2)}, \quad (8)$$

where:

$\theta_s, \theta_z$  - virtual potential temperature at the surface  $s$  and at the height  $z$ , respectively;

$u, v$  - horizontal wind components at height  $z$ ;

$g$  - gravitational acceleration.

The top of the boundary layer is given by the height at which the bulk Richardson number reaches a critical value. This approach could be improved for the stably stratified boundary layer following Zilitinkevich & Baklanov (2002).

### **Dry Deposition and Gravitational Settling**

Dry deposition is the removal of gaseous and particulate nuclides or other pollutants from the atmosphere to the earth surface by vegetation or other biological or mechanical means. It plays an important role for most nuclides (excluding the noble gases).

For the DERMA model, it was included via the mass loss due to dry deposition in the calculation of source term  $Q_p$  - the amount of radionuclide associated with each puff  $p$  depending on the emission rate (the so-called source depletion method). As a first simple parameterization of dry deposition we used a classic approach, based on the concept of the deposition velocity  $v_d$ . The dry deposition takes place in the lower surface layer and does not apply to the free troposphere ( $z > h$ ).

Therefore, using the assumption employed in the DERMA model about complete vertical mixing within the atmospheric boundary layer (ABL) for each  $p$  puff, we can obtain the following simple formula for the mass loss due to dry deposition:

$$Q_p|_{n+1} = Q_p|_n \exp\left(-\frac{\Delta t \cdot v_d}{h}\right), \quad (9)$$

where:

$\Delta t$  - time step of the model,

$h$  - mixing layer height.

*Prahm & Berkowicz (1978)* showed that the source depletion method can give considerable errors of the surface air concentration in case of stable stratification of the ABL. If an air pollution model can simulate the vertical structure/profile of concentration within the ABL, especially for the local scale, the surface depletion approach is more suitable for simulation of dry deposition. However, in case of using the approach of complete vertical mixing within ABL (as it is done in the DERMA model), the difference between both methods is not significant. Calculation of the radionuclide amount deposited on the surface due to dry deposition is performed at each time step.

The dry deposition velocity depends on many parameters describing particles and characteristics of the ground surface and surface layer. For the simplest case of dry deposition parameterization (in the emergency version of the DERMA model), we assume that the dry deposition velocity is a constant for each nuclide and surface type.

However, it should be noted that this parameterization is not very suitable for simulation of accidental releases, because numerous experimental studies (cf. e.g. an overview by *Baklanov & Sørensen (2001)*) showed that the dry deposition velocity depends on the size of the deposited particles. Therefore, for the dry deposition velocity of more than 300 radionuclides the different values were used in the DERMA model.

For particles, especially for heavy particles (radius  $r_p > 1 \mu\text{m}$ ), the gravitational settling strongly affects the process of deposition to the surface. The effect of gravitational settling, described through the gravitation settling velocity,  $v_g$ , is included in the dry deposition velocity value. For particles with diameter of less than  $4 \mu\text{m}$ , for which the airflow around the falling particle can be considered laminar, the gravitational settling velocity is given by Stokes' law (*Hinds, 1982*):

$$v_g = \frac{2C(\rho_p - \rho)gr_p^2}{9\nu}, \quad (10)$$

where:

$\rho_p, \rho$  - particle and air densities, respectively,

$g$  - gravitational acceleration,

$r_p$  - particle radius,

$\nu$  - kinematic viscosity of air ( $1.5 \cdot 10^{-5} \text{ m}^2/\text{s}$ ),

$C$  - Cunningham correction factor (*Zanetti, 1990*), which for small particles ( $r_p < 0.5 \mu\text{m}$ ) can be expressed:

$$C = 1 + \frac{\lambda}{r_p} \left[ a_1 + a_2 \exp\left(-\frac{2a_3 r_p}{\lambda}\right) \right], \quad (11)$$

where:

$\lambda$  - mean free path of air molecules ( $\lambda = 6.53 \cdot 10^{-5} \text{ m}$ ),

$a_1=1.257$ ,  $a_2=0.40$ , and  $a_3=0.55$  - constants.

### **Wet Deposition**

The Chernobyl accident showed that the wet deposition or pollutant scavenging by precipitation processes is very important for evaluation of the radionuclide atmospheric transport from nuclear accidental releases as well as estimation of the deposited radioactivity pattern. Usually the wet deposition is treated in a standard way with a washout coefficient for the below-cloud scavenging and a rainout coefficient for the in-cloud scavenging (Yamartino, 1985; Seinfeld, 1986; Zanetti, 1990).

As a first approximation for the emergency response version of the DERMA model, for parameterization of the wet deposition (absorption into droplets followed by droplet removal by precipitation) of aerosol particles or highly soluble gases, we can describe the local rate of material removal as the first-order process:

$$\frac{dc}{dt} = \Lambda(r_p, x_i, t) \cdot c(x_i, t) \quad (12)$$

where:

$\Lambda(r_p, x_i, t)$  - total scavenging (washout or rainout) coefficient (depends on the height above the surface and on the time).

The wet deposition flux to the surface, in contrast to the dry deposition flux, is the sum of wet removal from all volume elements aloft, assuming that the scavenged material comes down as precipitation. For the DERMA model, by using the assumption of complete vertical mixing within the ABL and assuming that the rain clouds are contained in ABL, we can express the wet deposition velocity as:

$$v_w = A' \cdot H_r, \quad (13)$$

where:

$A'$  - vertically averaged washout coefficient,

$H_r$  - the height of the cloud base.

In case of simulation without splitting the scavenging process in washout and rainout,  $H_r$  will be the height of the cloud top. Thus, we obtain a formula similar to Eq. (9) for the calculation of the mass loss by the wet deposition:

$$Q_p|_{n+1} = Q_p|_n \exp\left(-\frac{\Delta t \cdot H_r \cdot \Lambda'}{h}\right) \quad (14)$$

If the height of the rain cloud base  $H_r$  is unknown, one can assume that  $H_r = h$ .

As it was mentioned above, the scavenging coefficient  $\Lambda(r_p, x_i, t)$  includes the washout and rainout coefficients, and hence, it is possible to present it as a sum of two coefficients:  $\Lambda(r_p, x_i, t) = \Lambda_w(r_p, x_i, t) + \Lambda_r(r_p, x_i, t)$ . The washout and rainout mechanisms are spatially separated (the rainout is effective within the clouds, the washout below the clouds).

### **Washout**

The below-cloud scavenging (washout) coefficient,  $\Lambda_w$ , for aerosol particles of radius  $r_p$  can be expressed in a general form as:

$$\Lambda_w = -\pi N_r \int a^2 w_a(a) E(r_p, a) f_a(a) da, \quad (15)$$

where:

$N_r$  - total number of raindrops residing in a unit volume,

$a$  - raindrop projected radius,

$E(r_p, a)$  - aerosol capture efficiency term,

$w_a(a)$  - vertical velocity of the raindrops (negative if downward),

$f_a(a)$  - probability-density function of the raindrop size distribution.

The limits of integration are from the ground surface to the cloud base. The aerosol capture efficiency  $E(r_p, a)$  is a function of the radius of particle,  $r_p$ , and of rain drops,  $a$ , and depends upon several mechanisms mentioned by *Hales (1986)*:

- impaction of aerosol particles on the rain drop,
- interception of particles by the rain drop,
- Brownian motion of particles to the rain drop,
- nucleation of a water drop by the particle,
- electrical attraction,
- thermal attraction,
- diffusioforesis.

The washout coefficient,  $A_w$ , varies spatially and temporally. However, in order to simplify, one may use a vertically averaged washout coefficient,  $A_w'$ , below the clouds in combination with the surface precipitation data.

As it was shown (e.g. *Baklanov, 1999*), in most models of long-range pollution transport the washout coefficient does not depend on particle radius. However, as it is mentioned in an overview by *Baklanov & Sørensen (2001)*, the  $E(r_p, a)$  and correspondingly  $A_w$  are strongly depending on the particle size (the so-called “Greenfield gap”). According to experimental data (*Tschiersch et al., 1995; Radke et al., 1977*), the washout coefficient for particle radii in the range of 0.01–0.5  $\mu\text{m}$  is about of  $0.1 \cdot 10^{-3}$ – $0.5 \cdot 10^{-3} \text{ sec}^{-1}$ , and it is two orders of magnitude smaller than that for particles larger than 4  $\mu\text{m}$ .

Therefore, as a first approximation, *Baklanov & Sørensen (2001)* suggested a revised formulation of the vertically averaged washout coefficient for particles of different size:

$$\Lambda'(r_p, q) = \begin{cases} a_0 \cdot q^{0.79} & \text{if } r_p \leq 1.4 \mu\text{m} \\ (b_0 + b_1 r_p + b_2 r_p^2 + b_3 r_p^3) f(q) & \text{if } 1.4 \mu\text{m} < r_p < 10 \mu\text{m} \\ f(q) & \text{if } r_p \geq 10 \mu\text{m} \end{cases}, \quad (16)$$

$$f(q) = a_1 q + a_2 q^2,$$

where:

$q$  – precipitation rate (mm/h),

$a_0 = 8.4 \cdot 10^{-5}$ ,  $a_1 = 2.7 \cdot 10^{-4}$ ,  $a_2 = -3.618 \cdot 10^{-6}$ ,

$b_0 = -0.1483$ ,  $b_1 = 0.3220133$ ,  $b_2 = -3.0062 \cdot 10^{-2}$ , and  $b_3 = 9.34458 \cdot 10^{-4}$ .

The effects of particle size and rain intensity on the washout coefficient, as calculated by the revised formulation (16) were analyzed by *Baklanov & Sørensen (2001)* and it was shown that this formulation had a better correlation with the measurement data compared with the previous formulations (*Näslund & Holmström (1993)* and others), which did not consider effects of the particle size.

### **Rainout**

Beside washout below a cloud base, there are the following additional effects of wet deposition when air pollutants are transported inside clouds: 1) rainout between the cloud’s base and top (scavenging within the cloud), and 2) wet deposition caused by deposition by fog. The first process of rainout between the cloud base and top depends on the types of precipitation (i.e. convective or dynamic types).

The rainout coefficient for the convective precipitation is more effective/intensive than the washout coefficient, and it can be estimated (according to *Maryon et al. (1996)*) by the following formula:

$$A_r'(r_p, q) = a_0 q^{0.79}, \quad (17)$$

where:  $a_0 = 3.36 \cdot 10^{-4}$ . *Crandall et al. (1973)* showed simulations of different mechanisms for rainout in which the rainout coefficient was not a strong function of the particle size.

The rainout coefficient for the dynamic precipitation is approximately equal to the washout coefficient, and hence, the rainout effect in this case can be also estimated by Eq. (16).

### **Snow Scavenging**

According to recent publications (e.g. *Hongisto, 1998; Maryon & Ryall, 1996*) in most models the processes of scavenging by snow are described by the same formulae as for rain (e.g. Eqs. (14), (16), and (17) in our case), but with other values of the scavenging coefficient,  $A$ . The range of  $A$  values for snow is 2–10 times lower than the washout coefficient for rain with equivalent precipitation rates.

For scavenging by snow (according to *Maryon et al. (1996)*), the following simple formulation without any dependence of the coefficient  $A'$  on the particle radius could be used:

$$A_s'(q) = a_0 q^b, \quad (18)$$

where:  $a_0 = 8.0 \cdot 10^{-5}$  and  $b = 0.305$  for scavenging by snow below the cloud base and between the cloud base and top for dynamic precipitation; and  $a_0 = 3.36 \cdot 10^{-4}$  and  $b = 0.79$  for scavenging by snow between the cloud base and top for convective precipitation.

Unfortunately, the processes of scavenging by snow are not well studied. For example, there are effects of the water content in snowflakes on the scavenging by snow, especially for the air temperatures close to  $0^\circ\text{C}$  (*Karlsson & Nyholm, 1998*), but there is no relevant experimental data for this effect.

### **Radioactive Decay**

Radioactive decay transforms many basic dose contributing nuclides and should be taken into consideration for simulation of the possible radioactive contamination. The decay effects in the following ways:

- simple decay to non-radioactive elements;
- radioactive daughter nuclides (B, or B1, B2);
- secondary decay of daughter nuclides (C, D, etc.).

It is possible to split the DERMA modelling of the radioactive decay into two basic phases. The first phase is employed during the airborne transport of the short-living nuclides (like  $^{131}\text{I}$ ). The second phase is employed after the airborne transport is completed and the long-living (like  $^{137}\text{Cs}$ ) are deposited to the ground surface. This phase could be done in a separate subprogram/ submodel. For  $^{131}\text{I}$ , the simulation of physical and chemical form of nuclides includes three forms of iodine: gaseous forms - elemental iodine and organic iodine (e.g.,  $\text{CH}_3\text{I}$ ), aerosol form – iodine attached to aerosol particles. During the first week, the gaseous forms of  $^{131}\text{I}$  dominate. The dry deposition velocity,  $v_d$ , is corrected/ recalculated for 70% of gaseous  $^{131}\text{I}$ , and for the rest of the particles it is almost equal to  $v_d$  of  $\text{SO}_4$  particles.

The radioactive decay is taken into account through mother ( $A$ ) and possible daughter nuclides ( $B$ ,  $C$ , etc.) by the following formulae:

$$\begin{aligned} \frac{dA}{dt} &= -\lambda_a A, \\ \frac{dB}{dt} &= -\lambda_b B + \lambda_a A, \\ \frac{dC}{dt} &= -\lambda_c C + \lambda_b B, \end{aligned} \quad (19)$$

where  $\lambda_a$ ,  $\lambda_b$ , and  $\lambda_c$  are the decay constants for corresponding nuclides.

## **6.2. Input meteorological dataset**



The meteorological data from the European Centre for Medium-Range Weather Forecasts (ECMWF), Reading, UK are based on the ECMWF's global model forecasts and analyses (<http://www.ecmwf.int>) having a resolution up to  $0.5^\circ \times 0.5^\circ$  latitude vs. longitude and 3 hours time interval for both Northern and Southern hemispheres. It consists of the geopotential, temperature, vertical velocity, u and v components of horizontal wind, relative humidity and specific humidity at each level, etc. Analysis has been done on a daily basis at 00, 06, 12 and 18 UTC terms.

The ECMWF has the following data archives: ECMWF/WCRP level III-A Global Atmospheric Data Archive (TOGA), Operational Atmospheric Model, ERA-15 (ECMWF Re-Analysis 15), ERA-40 (ECMWF Re-Analysis 40), Wave Model, Ensemble Prediction System (EPS), Seasonal Forecast, and Monthly Means.

The ERA-15 production system generated re-analyses from December 1978 to February 1994. The ERA-15 Archive contains global analyses and short range forecasts of all relevant weather parameters, beginning with 1979, the year of the First GARP Global Experiment (FGGE). The Level III-B archive is subdivided into three classes of data sets: Basic  $2.5^\circ \times 2.5^\circ$  Data Sets (17 vertical pressure levels); Full Resolution Data Sets (e.g.  $1^\circ \times 1^\circ$ , 31 hybrid model vertical levels); Wave archive.

The data sets are based on quantities analyzed or computed within the ERA-15 data assimilation scheme or from forecasts based on these analyses. The Basic Data Sets contain values in a compact form at a coarse resolution. They are particularly suitable for users with limited data processing resources. The Full Resolution Data Sets provide access to most of the data from the ERA-15 atmospheric model archived at ECMWF. These archives have a higher space resolution. They should only be used where high resolution is essential; in this respect they are particularly suited for use in conjunction with case studies and as initial conditions for high-resolution models. This archive includes analysis, forecast accumulation and forecast data. Data are available on the surface, pressure levels and model levels.

The new reanalysis project ERA-40 (Simmons and Gibson, 2000) will cover the period from mid-1957 to 2001 overlapping the earlier ECMWF reanalysis, ERA-15, 1979-1993. Analysis and forecast fields will only be made available as complete years and only after validation.

In this particular study we used ECMWF data, available at DMI for the forecast mode or analyzed and archived mode. The horizontal resolutions of the meteorological data are different from year to year. For example, for the year 2000 the data have a resolution of  $1^\circ \times 1^\circ$  latitude vs. longitude and 6 hours time resolution. It consists of temperature, u and v components of horizontal wind, and specific humidity at each level, plus surface fields. Analyses have been done at 00 and 12 UTC.

### 6.3. Selected assumptions for long-term simulations

The suggested approach for long-term modelling can be realized practically by the following ways of using NWP data: (i) simulations from meteorological data archives, (ii) every day real-time runs using analyzed NWP model data available in the NWP database followed by archiving of the dispersion simulation data. Certain national meteorological services, e.g. SMHI, perform daily forecasting of atmospheric dispersion from hypothetical accidental releases from a number of NPPs. Such data could be archived for long-term statistical risk analyses. However, the quality will be lower than for the results based on analyzed NWP data.

The simulated fields of the air contamination and deposition on the surface by this approach of the long-term dispersion modelling can be used and interpreted as:

- (i) long-term effects (accumulated or average contamination) of existing continuous release sources (ventilation emission from risk sites (e.g., 129I from Sellafield, noble gases from nuclear plants), natural radioactivity emission (e.g., Rn products), industrial pollution etc.);
- (ii) probabilistic characteristics of possible radioactive contamination of different territories in case of an accident at an NRS.

For this particular study of the Arctic Risk project, we followed several basic assumptions in

practical simulations.

- First, for simplicity, we selected for risk sites the continuous “unit discrete hypothetical release” (UDHR) of radioactivity ( $1 \cdot 10^{10}$  Bq/s) with discrete emitting of puffs (every 60 minutes) during 24 hours. Hence, in this case the total amount of radioactivity released during one-day release is equal to  $8.64 \cdot 10^{11}$  Bq.
- Second, we considered only one radionuclide  $^{137}\text{Cs}$ , as a radionuclide of key importance. Although the calculation might be done for any of more than 300 radionuclides incorporated into the database of the DERMA model.
- Third, the simulation was performed during one full year (1 Jan – 31 Dec) on a daily basis considering the length of the 10-day trajectories (i.e. after release of radioactivity occurred from the site the tracking of the radionuclide cloud was limited to 10 days of atmospheric transport from each site). The period of calculation of long-range atmospheric transport of  $\text{Cs-137}$  was given from 1 January to 31 December (reference year of 2000).
- Fourth, to minimize the computing resources used for the dispersion modelling approach, we selected only one year in our study, although it should be noted that for the statistical analysis the multiyear period is more preferred.
- Fifth, using the DERMA model, we calculated several important characteristics. Among these characteristics are the following:
  - air concentration (Bq/m<sup>3</sup>) of the radionuclide in the surface layer – surface air concentration field,
  - time-integrated air concentration (Bq·h/m<sup>3</sup>) of the radionuclide in the surface layer – integral air concentration at surface field,
  - dry deposition (Bq/m<sup>2</sup>) of the radionuclide on the underlying surface – dry deposition field, and
  - wet deposition (Bq/m<sup>2</sup>) of the radionuclide on the underlying surface – wet deposition field.
- Since in calculations it was assumed that capacity of each source was equal to a conventional value of  $10^{11}$  Bq/s, the transformation from this conventional value to real values was made at the stage of post-processing of modeling results. The authors used directly proportional dependence of surface  $\text{Cs-137}$  activity on the source power. The real power value was calculated by the data of erosion ability of soil cover and  $\text{Cs-137}$  surface activity in the epicenters of carrying-out of radioactive aerosols. It was assumed that the fraction of mobile forms of  $\text{Cs-137}$  in soil was 10%. In autumn-winter period when sources of wind transport are either covered with snow or their soil is frozen the source power was taken equal to zero.

## 6.4. Post-processing of concentration and deposition fields

In order to adapt model DERMA to the conditions of Semipalatinsk test site a special data package was formed. This package included the map of the test site and adjacent territory, the map of test site area contamination with radionuclides by the results of modeling for the full year, and the map of epicenters of possible carrying-out of radioactive aerosol.

Model DERMA gave a large amount of information which was processed using special complex of programs developed within GIS-project MigRad. The scheme of sequence of post-processing of the results of modeling with names of program blocks is shown in Figure 22. To introduce the results of modeling into GIS-project MIGRAD and to carry out analysis the following procedures were used:

- Procedure `derma2.exe` – extraction from the archive, sorting, averaging and formation of package of files each of which refers to modeling of one day of calculated period. This procedure was developed because DERMA is a trajectory, Lagrangian-type model, and results are loaded in the archive as a set of trajectories for the 14-day period and shift of the beginning of calculations successively by 1 day.
- procedure `txt2grid_proj.aml` converting ASCII files in grids, making coordinate adjustment

- and transformation of projections;
- Procedure `average_year.aml` calculating average monthly and average annual fields of concentrations of radioactive aerosol and its precipitation on underlying surface.

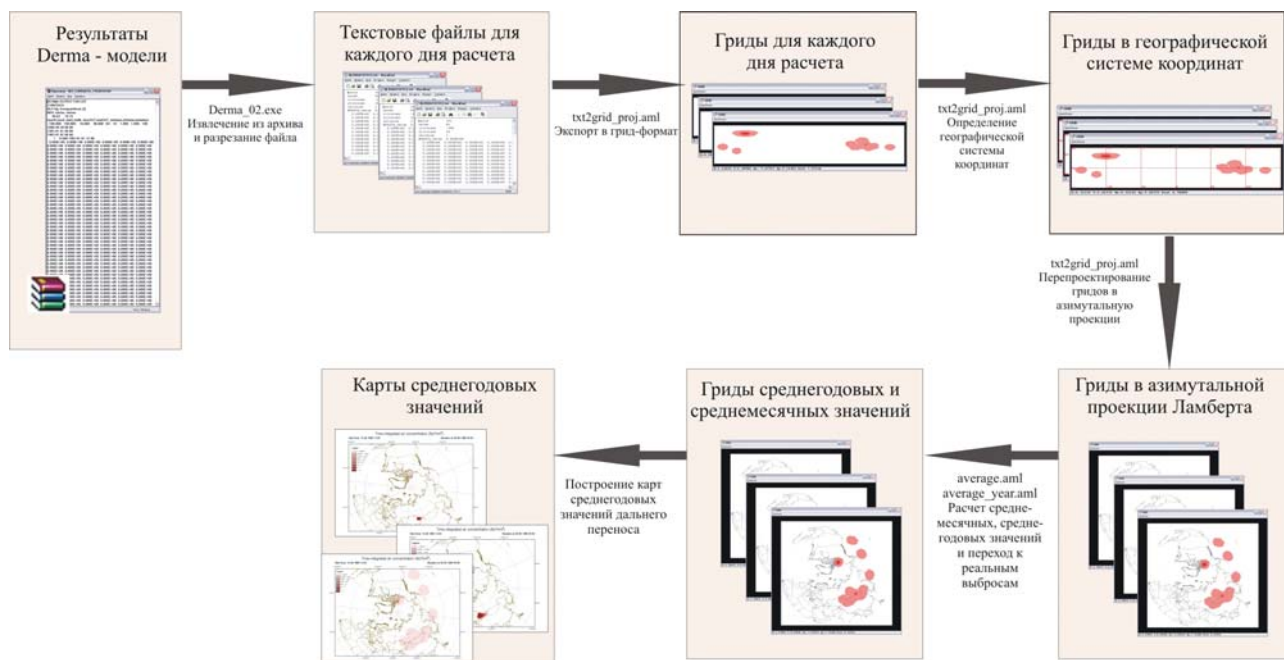


Figure 22. Scheme of post-processing of model DERMA results

## 6.5. Integration of modelling results into GIS environment

Calculation of long-range transfer of CS-137 enabled to obtain the following results:

- concentration in atmosphere ( $\text{Bq}/\text{m}^3$ );
- dry deposition ( $\text{Bq}/\text{m}^2$ );
- wet deposition ( $\text{Bq}/\text{m}^2$ ).

The Figure 23 visualizes average annual results of modeling as a diagram of 5 cities: Astana, Almaty, Semipalatinsk, Novosibirsk (Russia) and Uliastau (Mongolia). Though Astana is at a smaller distance (about 600 km) from the STS site than Novosibirsk (about 650 km), the values of concentration of dry, wet and summarized precipitations modeled for Novosibirsk are an order of magnitude higher than those in Astana. In Almaty-city situated at a distance of 750 km from the test site Cs-137 pollution must be ten times less than in Astana. Calculations give the lowest level of pollution in Uliastau and the highest – in Semipalatinsk.

Figure 24 (see also Figs. in Appendices A-B for two other sites) illustrate the results of calculations of spreading in the atmosphere, dry and wet precipitation of radionuclide Cs-137. The figures show average annual fields of the above quantities for three sources situated in the vicinity of testing grounds Experimental field, Degelen and Balapan. As it is seen from the figures radioactive substances are transported at large distances with prevailing transport in eastern and north-eastern directions. It means that during the tests the risk of radioactive pollution was higher in northern areas of Kazakhstan, Siberia and Altay, which is confirmed by earlier investigations by *Tleuber-genov (1997)*.

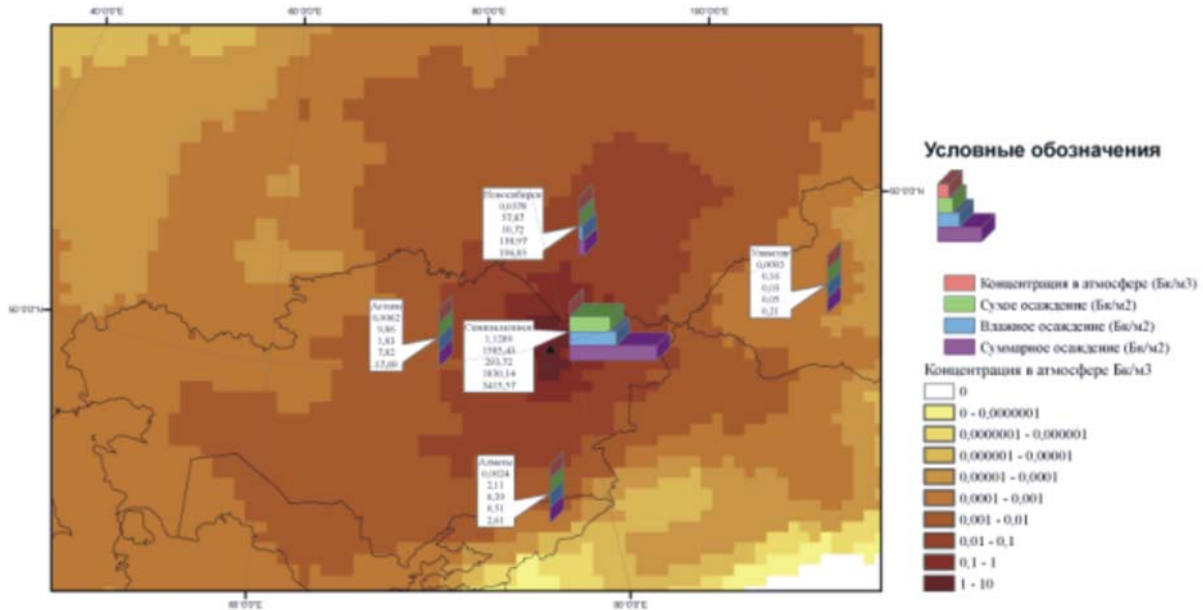


Figure 23. Results of modeling of transboundary transport with diagrams for 5 cities.

Therefore, GIS-project MigRad designed as instrument for analysis of complex territorial processes” awakened” by numerous tests of nuclear devices on the territory of Semipalatinsk test site provides the following possibilities:

- visual analysis of extensive cartographic material, remote sensing data and data of field measurements collected in the corresponding databases;
- modeling of radionuclide migration with rain flows using the model of redistribution and accumulation of soil particles;
- analysis of thermal anomalies which arose on the test site territory and adjacent territories caused by test explosions,
- modeling of long-range transport of radioactive aerosols with analysis of dynamics of their spreading, average annual concentration fields, dry and wet (rain, snow) precipitation.

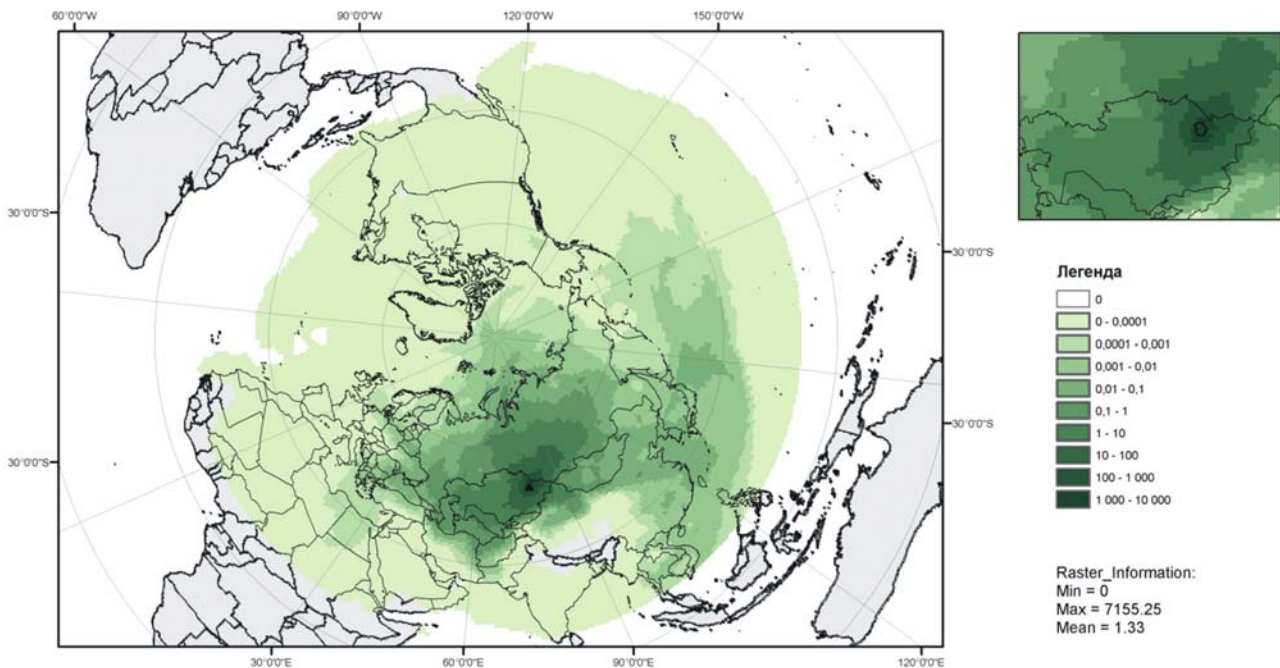
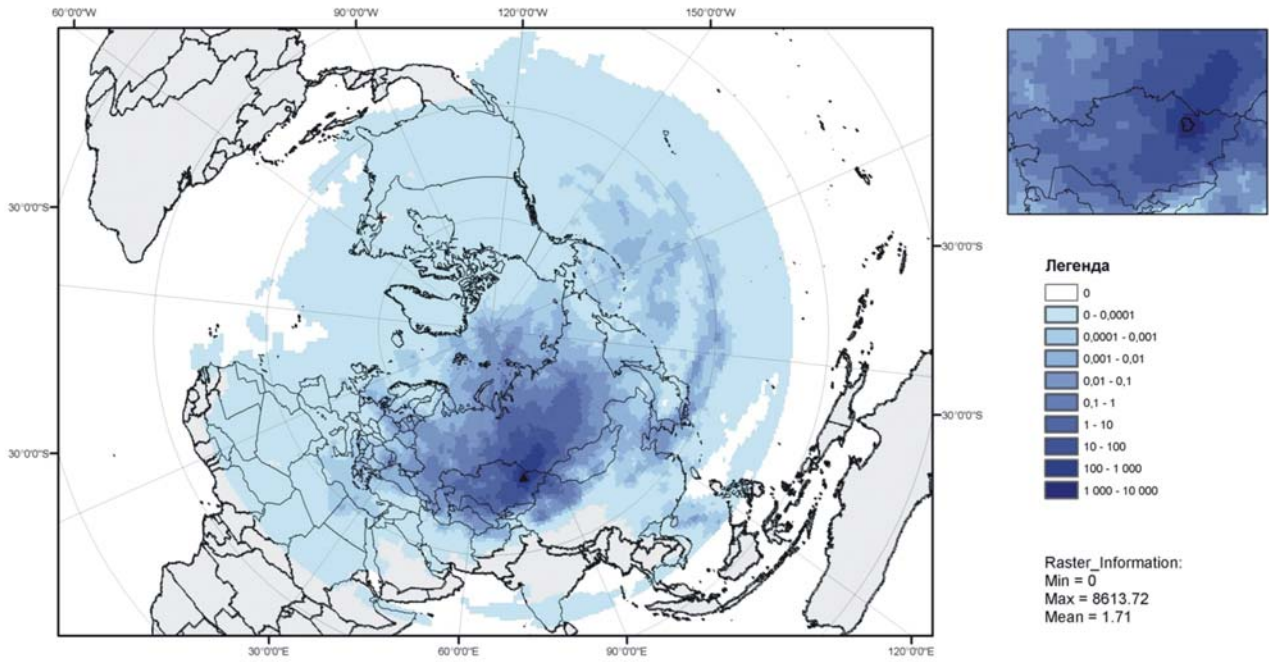
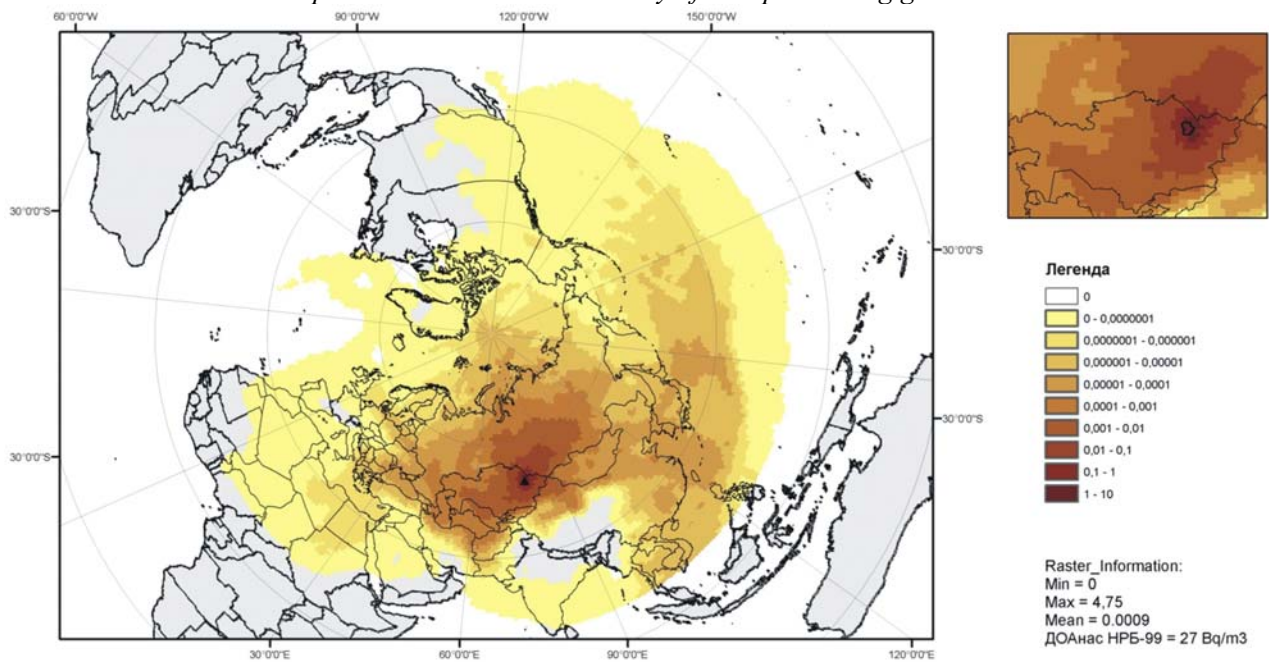


Figure 24a. Average annual dry deposition of Cs-137 (Bq/m<sup>2</sup>) of radioactive pollution spreading from the epicenter located in the vicinity of Balapan testing ground.



**Figure 24b.** Average annual wet deposition of Cs-137 ( $Bq/m^2$ ) of radioactive pollution spreading from the epicenter located in the vicinity of Balapan testing ground.



**Figure 24c.** Average annual concentration of Cs-137 ( $Bq/m^3$ ) of radioactive pollution spreading from the epicenter located in the vicinity of Balapan testing ground.

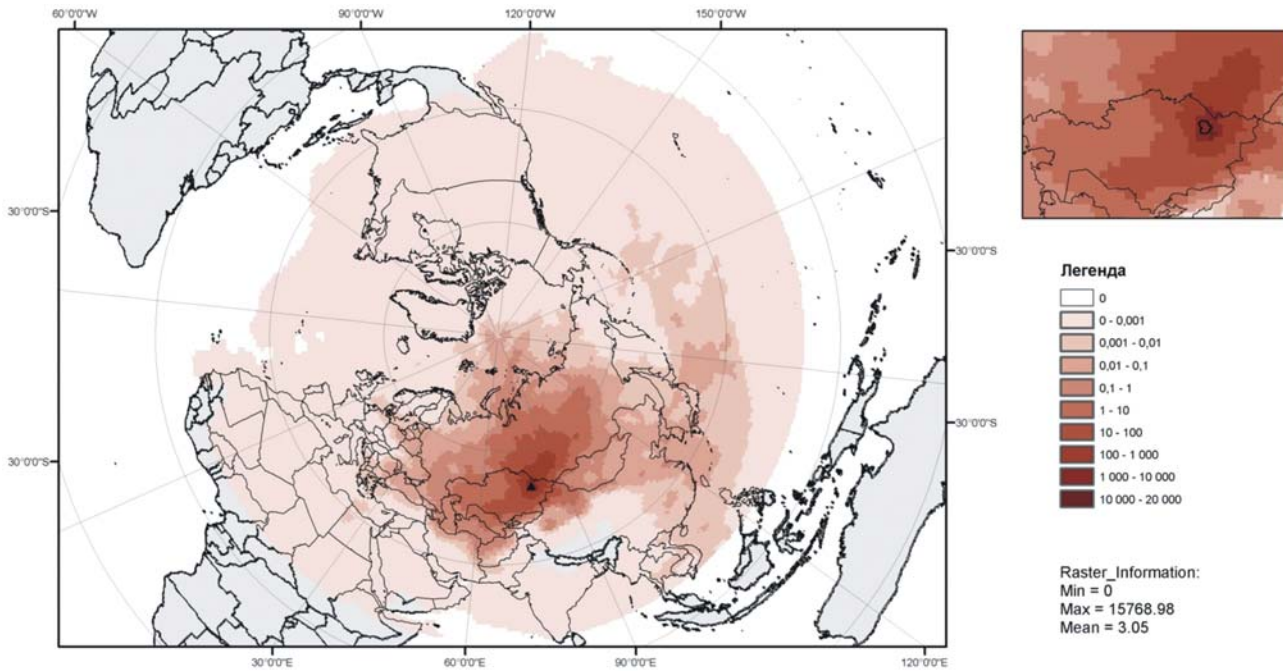


**Figure 24d.** Average annual total deposition of Cs-137 (Bq/m<sup>2</sup>) of radioactive pollution spreading from the epicenter located in the vicinity of Balapan testing ground.

## Conclusions

In this study we developed, tested and applied the software complex as the GIS-project MigRad (Migration of Radionuclide) oriented at integration of a large volume of various information (mapping, ground-based and satellite-based survey) and modeling on its base local redistribution of radionuclides by rain flows and long-range transfer of radioactive aerosol from the territory of the Semipalatinsk test site/ polygon (Republic of Kazakhstan). Since 1961, in total 348 underground nuclear explosions were made on the territory of the test site. The thermal anomaly on territory of the polygon was investigated, and the object-oriented analysis was employed for the studied area. Employing the RUNOFF model, the simulation of radionuclides migration with surface waters was performed. Employing the DERMA model, the simulation of long-term atmospheric transport dispersion and deposition patterns for cesium was conducted from 3 selected test sites (Balapan, Delegen, and Experimental Field) was conducted. Employing GIS technology, the mapping of the of the high temperature zones and epicenters of radioactive aerosol transport for the territory of the test side was carried out with post-processing and integration of modelling results into GIS environment. Contamination levels of pollution due to former nuclear explosions for population and environment of the surrounding polygon areas of Kazakhstan as well as adjacent countries were analyzed and evaluated.



## References

- Akhmetzhanov A.Kh., L.A. Kazamirchuk. Numerical analysis of meteorological fields on the territory of Kazakhstan on the base of geoinformational system // Abstracts of International conference "ENVIRONMENT 2000". - Tomsk, 2000. – pp. 38-39.
- AR-NARP (2005) Atmospheric Transport Pathways, Vulnerability and Possible Accidental Consequences from the Nuclear Risk Sites in the European Arctic (Arctic Risk) Project of the NARP: Nordic Arctic Research Programme. DMI project web site: <http://www.dmi.dk/f+u/luft/eng/arctic-risk/main.html>.
- Atlas. Radioecological situation on the territory of the Republic of Kazakhstan from 1954 to 1994. - Almaty: Ministry of Ecology and Bioresources, RK, 1997. V. 16, Semipalatinsk oblast – p. 400.
- Baklanov A, J.H. Sørensen, A. Mahura. Long-Term Dispersion Modelling: Part I: Methodology for Probabilistic Atmospheric Studies. / J. of Computation Technologies. - 2006. – Vol. 11. – P. 136-156.
- Baklanov A., Mahura A., Sorensen J.H. Long-term dispersion modeling. Part 1: Methodology for probabilistic atmospheric studies // Computational technologies. - 2006. – v. 1, part 1. – pp. 136-156.
- Baklanov A., Sørensen J.H., (2001) Parameterization of radionuclide deposition in atmospheric dispersion models. Phys. Chem. Earth, (B), 26, 787–799.
- Baklanov, A. (1999) Parameterization of the deposition processes and radioactive decay: A review and some preliminary results by the DERMA model. DMI Scientific Report, No. 99-4. 40 pp.
- Balakay L.A. Geoinformation Modeling of Radio-Nuclides Transfer Process// Abstracts of International Conference “Mathematical Modeling of Ecological Systems”. – Almaty, 2003. – P. 44
- Balakay L.A. Zoning of hazardous territories of Semipalatinsk nuclear test site// Abstracts of international scientific-practical conference “Sovereign Kazakhstan: 10 years of development of space research”. - Almaty, 2001. – p. 14
- Bocharov V.S., S.A. Zelentsov, V.N. Mikhaylova. Characteristics of 96 underground nuclear explosions on the STS // Atomic energy. - 1989. - v. 67, is. 3. – pp. 210-214.
- Climate USSR. Reference-book. Climate of the USSR. Ed..Veter. - L.: Gydrometeoizdat, 1967. – p.170.
- Crandall, W.K., C.R. Molenkamp, A.L. Williams, M.M. Fulk, R. Lange & J.B. Knox (1973) An investigation of scavenging of radioactivity from nuclear debris clouds: research in Progress. Lawrence Livermore National Laboratory, California, USA, Report UCRL-51328.
- Derbentsova A.M. Soil erosion and protection (Mechanical degradation of soils). - Vladivostok: Izd. Dalnevost. University, 2006. – p.88.
- Dubasov Yu.V. Present-day radiation situation on the former SEMIPALATINSK test site and on the adjacent territories. 1. Some results of the 1994 control-methodological survey // Radiochemistry. – 1997 - v. 39, is.1. – p. 80-88.
- ERDAS IMAGINE. Tour Guides. - Atlanta, Georgia: ERDAS, Inc., 1999 - 636 p.
- Foster G.R. Sediment yield from farm fields: The universal soil loss equation and Onfarm 208 plan implementation. In universal soil loss equation: past, present and future // Soil science society of America special publication. Soils science of America - Madison, Wis., 1979.- № .8. - P. 17-24.
- Galperin M.V., M. Sophiyev, A. Gusev, O. Aphinogenova. Approaches to modeling of transboundary pollution of European atmosphere by heavy metals/ Report EMEP/MCII-B. - M., 1995. – p.85. – No. 7/95.
- Gifford, F.A. (1984) The random-force theory: Application to meso- and large-scale atmospheric diffusion. Boundary-Layer Meteorology, 30: 159-175.
- Graziani, G., W. Klug & S. Moksa 1998: Real-Time Long-Range Dispersion Model Evaluation of the ETEX First Release. EU JRC.
- Haith D.A., Tubbs L.J., Pickering N.B. Simulation of pollution by soil erosion and soil nutrient loss. - Pudoc Wageningen, 1984. - 66 p.
- Hales, J.M. (1986) The mathematical characterisation of precipitation scavenging. In: The Handbook of Environmental Chemistry / O. Hutzinger, editor, Vol. 4, Part A, pp. 149- 217.
- Henson U.S. (Eds). Transuranium elements in the environment. M.: Energoizdat, 1985. – p. 344.
- Hinds, W.C. (1982) Aerosol Technology. Wiley, New York. pp. 38-68 & 211-232.
- Hongisto, M. (1998) HILATAR, A regional scale grid model for the transport of sulphur and nitrogen compounds. Description of the model. Simulation results for the year 1993. Finnish Meteorological Institute, Helsinki, No 21.
- Ishikawa H. Evaluation of the Effect of horizontal diffusion on the long-range atmospheric transport simulation with Chernobyl data // Journal of applied meteorology, 1995. – Vol. 34, № 7. – P. 1653 – 1665.



- Karlsson, E. & Nyholm, S. (1998) Dry deposition of toxic gases to and from snow surfaces. *Journal of Hazardous Materials*, 60: 227-245.
- Klug, W., Graziani, G., Grippa, G., Pierce, D., Tassone, C. Evaluation of long range atmospheric transport models using environmental radioactivity data from the Chernobyl accident. EUR 14148 EN. Elsevier, 1992. – 54 p.
- Kuznetsov M.S., G.P. Glazunov. Soil erosion and protection. - M.: Izd. MSU, 1996. – p. 335.
- Kuznetsov M.S. To the problem of methods of studying soil erodibility // *Soil erosion and riverbed processes*. - 1973. - is. 3. - pp. 126-134.
- Larionov G.A. Soil erosion and deflation. - M.: MSU, 1993. – p.200.
- Lauritzen B., Mikkelsen T. A probabilistic dispersion model applied to the long-range transport of radionuclides from the Chernobyl accident // *Atmospheric Environment*, 1999. – Vol. 33. – P. 3271–3279.
- Logachev V.A. Semipalatinsk test site. Ensuring general and radiation safety of nuclear tests. M.: Second printing house FU “Medbioextrem” at Minzdrav RF, 1997. – p. 318.
- Mahura A., Baklanov A., Sorensen J.H. Long-term dispersion modeling. Part 2: Assessment of atmospheric transport and deposition patterns from nuclear risk sites in Euro-Arctic Region // *J. of Computation Technologies*. - 2005. – Vol. 10. – P. 112-134.
- Maryon R.H., D. B. Ryall, (1996) Developments to the UK nuclear accident response model (NAME). Department of Environment, UK Met. Office. DoE Report # DOE/RAS/96.011.
- Mirtzhulava Ts.E. Engineering methods of calculations and prognosis of water erosion. - M., Nauka, 1970. – p.239.
- Mirtzhulava Ts.E. Methods of prognosis of water erosion, solid runoff and ways of their development. // *Proc. IV All-Union Hydrolog. Conference. Riverbed processes*. – Leningrad, 1976. - v. 10. - pp. 132-139.
- Näslund, E. and Holmström, H. (1993) Inclusion of a three-dimensional washout coefficient in ADPIC. Report UCRL -ID-114054, Lawrence Livermore National Laboratory, California, USA.
- Ograsky H.O., Mockus V. Hydrology of agricultural lands. In: V.T. Chow (Ed.): *Handbook of applied hydrology*. - New York: McGraw-Hill. – Chapter 21.
- Prahm, L.P. & R. Berkowicz (1978) Predicting concentration in plumes subject to dry deposition. *Nature*, 271, 232-234.
- Radke, L.F., E.E. II Hindman & V.P. Hobbs. (1977) A case study of rain scavenging of aerosol particles from an industrial plume. *Proc. Symp. On Precipitation Scavenging, 1974. ERDA Symp. Series. NTIS*, pp. 425-436.
- Rambo J., Blakha M., UML 2.0. Object-oriented modelling and development. 2<sup>nd</sup> Edition, St. Petersburg, PITER, 2007. 544 p.
- Schopp W., Amann M., Cofala J., Heyes Ch., Klimont Z. Integrated assessment of European air pollution emission control strategies // *Environmental modeling and software*. – 1999. – Vol. 14, № 1. – P. 1-9.
- Schwertman U., Vogl W., Kainz M. Bodenerosion durch Wasser. Vorhersage des Abtrags und Bewertung von Gegenmaßnahmen. - Stuttgart: Ulmer, 1990. – 205 p.
- Seinfeld, J.H. (1986) *Atmospheric chemistry and physics of air pollution*. A Wiley-Interscience Publication. New-York.
- Shvebs G.I. Formation of water erosion, drainage of sediments and their assessment (on the example of Ukraine and Moldavia). - L.: Gydrometeoizdat, 1974. – p. 184.
- Shvebs G.I. Theoretical bases of erosion science. – Kiev, Odessa, 1981. – p. 224.
- Simmons, A.J. & Gibson, J.K., Eds. (2000) ERA-40 Project Report series. 1. The ERA-40 Project Plan. ECMWF, 62p.
- Smith, F. (1998) Estimating the Statistics of Risk from a Hazardous Source at Long Range, *Atmospheric Environment*, 32(16): 2775-2791.
- Smith, F.B. (1968) Conditioned particle motion in a homogeneous turbulent field. *Atmos. Environ.* 2, 491-508.
- Sørensen, J.H. (1997) Sensitivity of DERMA to boundary-layer parameters, and evidence for meso-scale influence on long-range transport. In: *ETEX Symposium on Long-range Atmospheric Transport, Model Verification and Emergency Responds*. Ed. K. Nodop, Vienna, Austria, 13-16 May 1997, EUR 17346 EN, pp. 207-210.
- Sørensen, J.H. (1998) Sensitivity of the DERMA Long-Range Gaussian Dispersion Model to Meteorological Input and Diffusion Parameters. *Atmos. Environ.* 32, 4195-4206.
- Sørensen, J.H., A. Rasmussen (1995) Calculations performed by the Danish Meteorological Institute. In:



- Report of the Nordic Dispersion/Trajectory Model Comparison with the ETEX-1 Fullscale Experiment. Eds. Tveten, U. and Mikkelsen, T., Risø-R-847(EN), NKS EKO-4(95)1, pp. 16-27.
- Sørensen, J.H., A. Rasmussen, T. Ellermann and E. Lyck (1998) Mesoscale Influence on Long-range Transport; Evidence from ETEX Modelling and Observations, *Atmospheric Environment*, 32, 4207-4217.
- Sørensen, J.H., Rasmussen, A. and Svensmark, H. (1996) Forecast of Atmospheric Boundary-Layer Height for ETEX Real-time Dispersion Modelling, *Phys. Chem. Earth*, 21, No. 5-6, 435-439.
- Strilchuk YU.G., L.D. Ptitskaya, A.Yu. Osintsev, V.N. Larin, A.V. Mityayev. Radiation situation in the places of underground nuclear explosions on testing grounds Balapan and Delegen of Semipalatinsk test site.
- Sultangazin U.M., Zakarin E.A., Spivak L.F., Arkhipkin O.P., Muratova N.R., Terehov A.G. Monitoring of temperature anomalies in the former Semipalatinsk nuclear test site // *Metrology instrumentation. C.R. Acad. Sci. – Paris*, 1998. T. 326. Serie II b. P. 135-140.
- Tarabrin N.P. Methods of determining erosion index of rains. Mechanisms of manifestation of erosion and riverbed processes in different natural conditions. // *Abstracts of II All-Union Interuniversity conf. – M.*, 1976. - pp. 55-57.
- Tleubergenov S.T. Test sites of Kazakhstan. - *Almaty: Gylym*, 1997. – P.745.
- Tschiersch, J., F. Trautner and G. Frank. (1995) Deposition of atmospheric aerosol by rain and fog. In: EC 'Radiation Protection' Report # EUR 16604 EN, pp. 3-11.
- Turganbayev E.S., L.A. Kazamirchuk. Geoinformational system of Semipalatinsk nuclear test site // *Materials of scientific-technical seminar "Contemporary information technologies and telecommunications: corporative information systems. Problems, perspectives of development, practical solutions. – Almaty*, 1999, 166 p.
- Turganbayev E.S., L.A. Kazamirchuk. Means of modeling and data manipulations in ARCINFO environment // *Materials of international scientific-practical conference "Problems of computational mathematics and information technologies". – Almaty*, 1999. – p. 363
- Turganbayev E.S., N.V. Saib, L.A. Kazamirchuk. Development and usage of three-dimensional models in GIS of Semipalatinsk nuclear test site// *Materials of scientific-technical seminar "Contemporary information technologies and telecommunications: corporative information systems. Problems, perspectives of development, practical solutions. – Almaty*, 1999. - p. 165
- Van Dop H., Addis R., Fraser G. ETEX: a European tracer experiment: observations, dispersion modeling and emergency response // *Atmospheric Environment*, 1998. – Vol. 32 (24). – P. 4089–4094.
- Vinogradova A.A., V.A. Yegorov. On possibility of long-range atmospheric transfer of pollutions to Russian Arctic zone // *Izv. As FAO*. - 1996. - v. 32. No 6. - pp. 796-802.
- Wischmeier W.H., Mannering J.V. Relation of soil properties to its erodibility // *Proc. Soil Sci.Am.* – 1969. - Vol. 33. - P. 131-137.
- Wischmeier W.H., Smith D.D. Predicting rainfall erosion losses. A guide to conservation planning // *Agricultural handbook prepared by science and education administration for U.S. Department of agriculture. – Washington*, 1978. - № 537. – 124 p.
- Yamartino, R.J. (1985) Atmospheric pollutant deposition modelling. Chapter 27 in: *Handbook of applied meteorology*. Houghton, D.D., Editor. A Wiley-Interscience Publication. New-York. 754-766 pp.
- Zakarin E., L. Spivak. E. Turganbayev, N. Muratova. Geoinformational system of Semipalatinsk nuclear test site. // *Arcreview*. – 1998. – No. 3 (6) – p. 10-12.
- Zakarin E.A., E.S. Turganbayev, L.A. Balakay. Geoinformational modeling on the territory of Semipalatinsk nuclear test site // *Izvestiya MES, NAS RK, series physics-math.* – 2003. – Special ed. No. 6, 111-119
- Zakarin E.A., L.A. Balakay. Designing of geoinformational system of Semipalatinsk nuclear test site. *Space research in Kazakhstan / Editor: U.M. Sultangazin. – Almaty, ROND*, 2002. – pp. 226-232.
- Zakarin E.A., L.A. Balakay. Geoinformational modeling and remote sensing of the territory of Semipalatinsk nuclear test site.// *Abstracts of International conference "Computer-Informational technologies for environmental sciences CITES – 2003". – Tomsk*, 2003. – p. 38
- Zakarin E.A., L.A. Balakay. Geoinformational modeling of radionuclide migration.// *Vestnik NNC RK, Geophysics and nonproliferation problems. Radioecology and environment protection*. 2003 (3), 44-47
- Zanetti, P. (1990) *Air Pollution Modeling - Theories, Computational Methods and Available Software*. Southampton: Computational Mechanics and New York: Van Nostrand Reinhold.
- Zilitinkevich, S. and A. Baklanov, 2002: Calculation of the height of stable boundary layers in practical applications. *Boundary-Layer Meteorology*, 105(3): 389-409.
- Zvonkov V.V. *Water and wind land erosion. – M.: Science*, 1963. – p.174.

## Appendix A: Radioactive pollution from Delegen test site

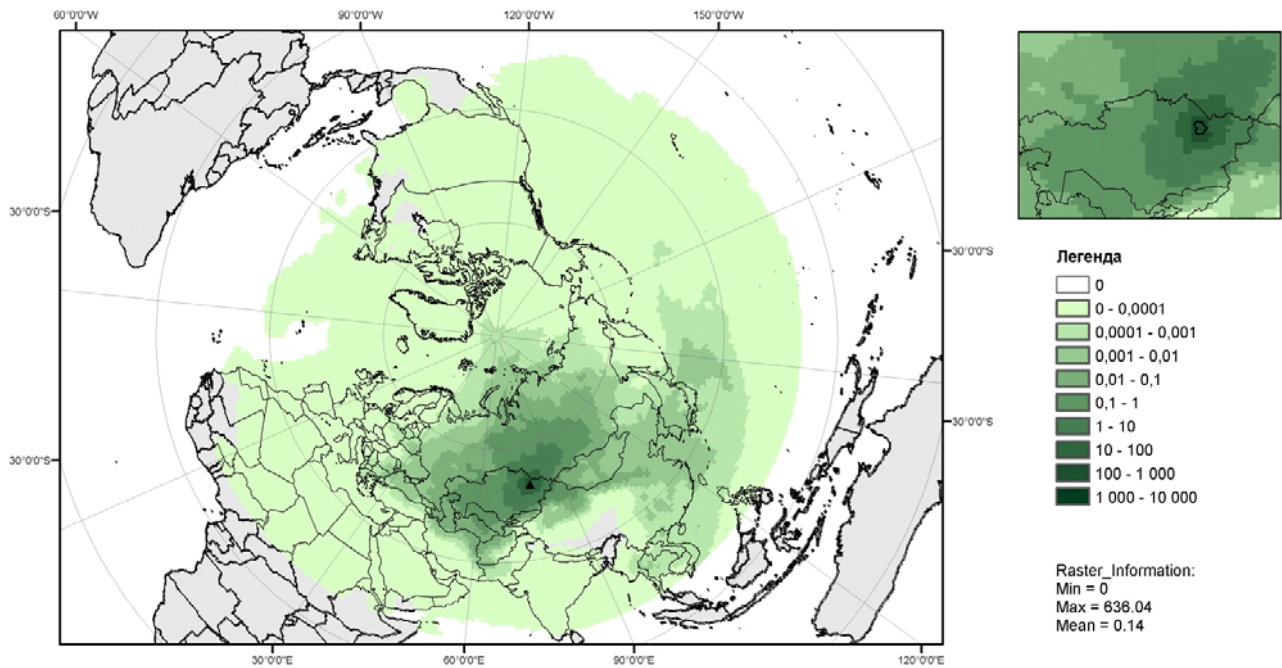


**Figure A1.** Average annual dry deposition of Cs-137 (Bq/m<sup>2</sup>) of radioactive pollution spreading from the epicenter located in the vicinity of Delegen testing ground

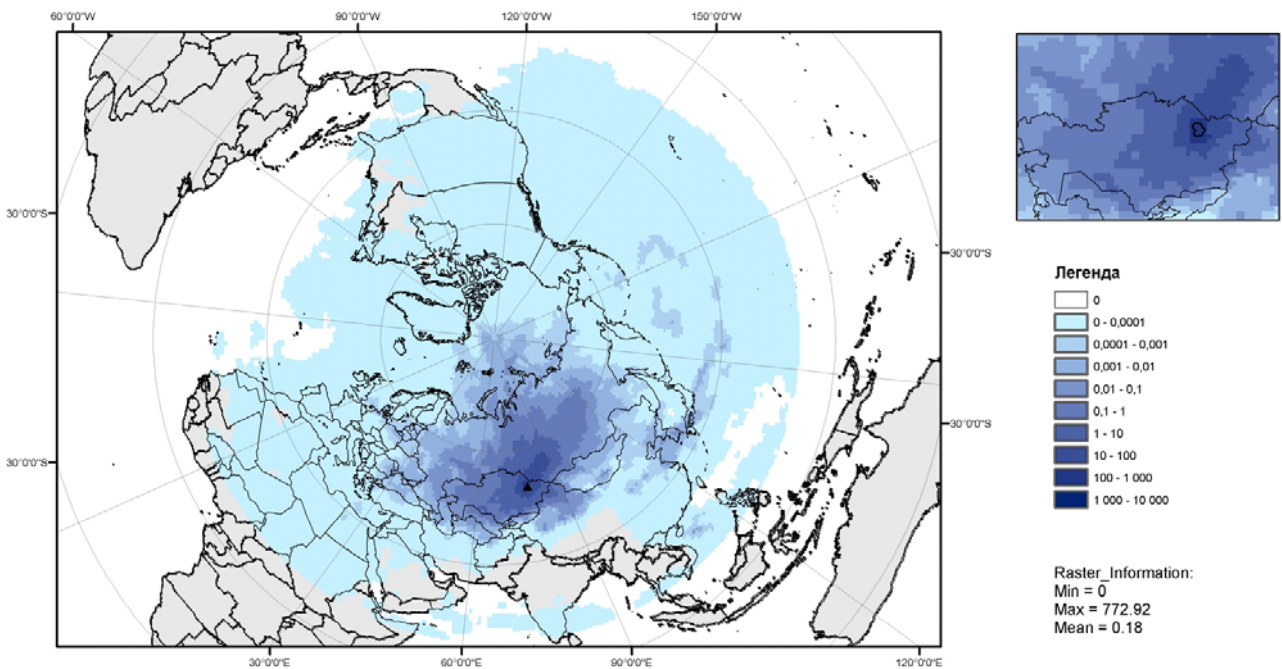


**Figure A2.** Average annual wet deposition of Cs-137 (Bq/m<sup>2</sup>) of radioactive pollution spreading from the epicenter located in the vicinity of Delegen testing ground

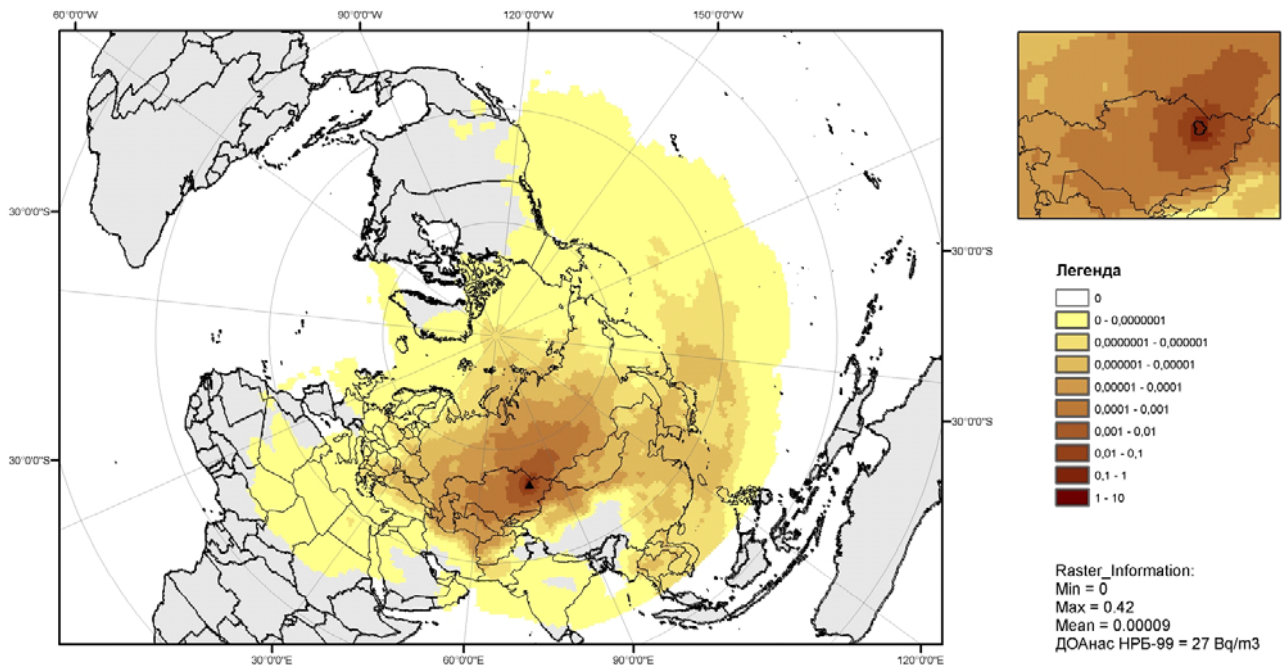


**Figure A3.** Average annual concentration of Cs-137 (Bq/m<sup>3</sup>) of radioactive pollution spreading from the epicenter located in the vicinity of Delegen testing ground.

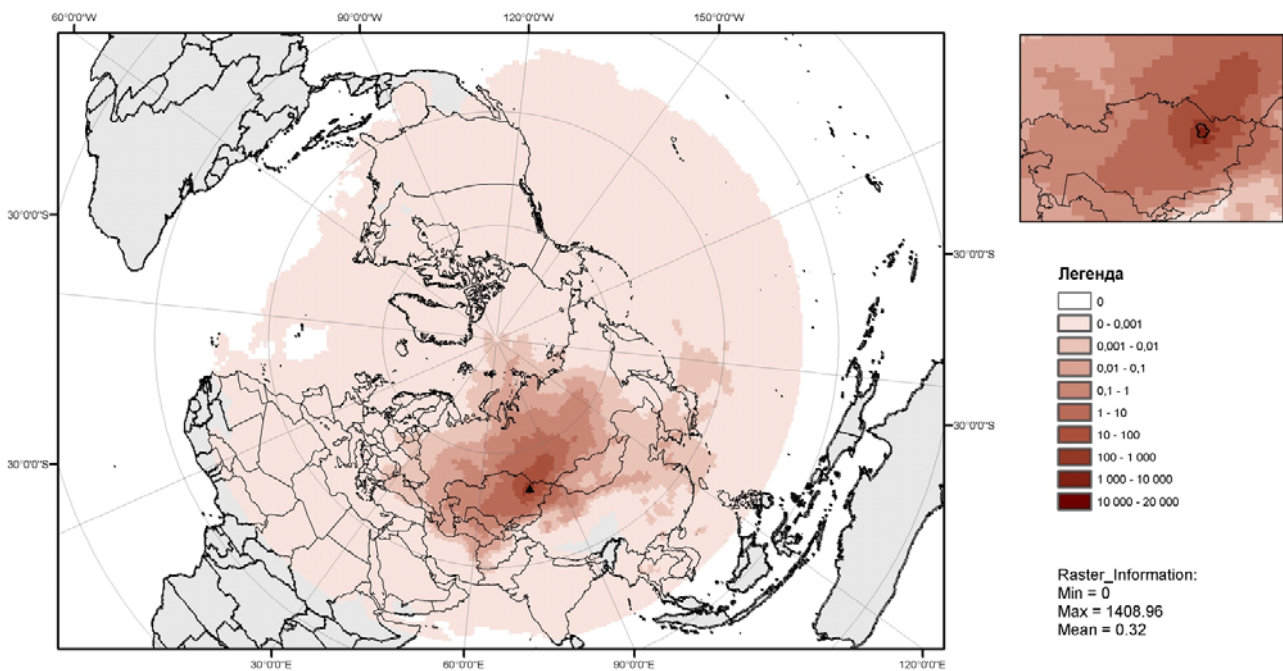


**Figure A4.** Average annual total deposition of Cs-137 (Bq/m<sup>2</sup>) of radioactive pollution spreading from the epicenter located in the vicinity of Delegen testing ground.

## Appendix B: Radioactive pollution from Experimental Field test site

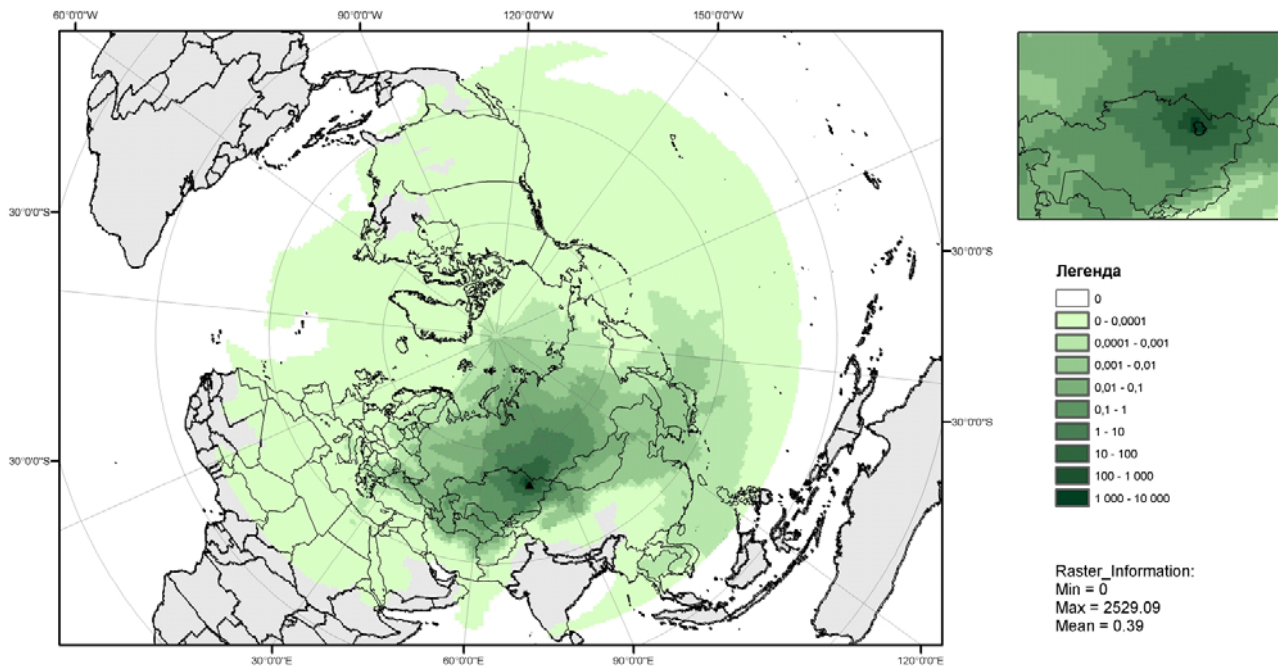


**Figure B1.** Average annual dry deposition of Cs-137 ( $Bq/m^2$ ) of radioactive pollution spreading from the epicenter located in the vicinity of testing ground Experimental Field

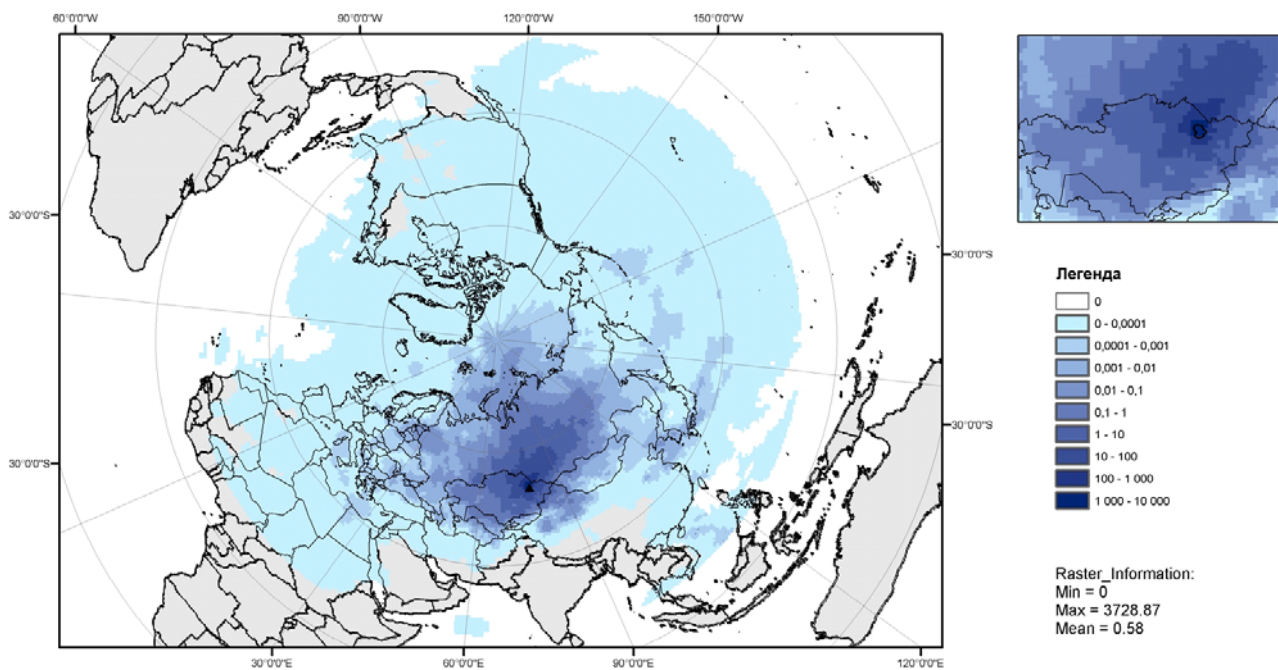


**Figure B2.** Average annual wet deposition of Cs-137 ( $Bq/m^2$ ) of radioactive pollution spreading from the epicenter located in the vicinity of testing ground Experimental Field.

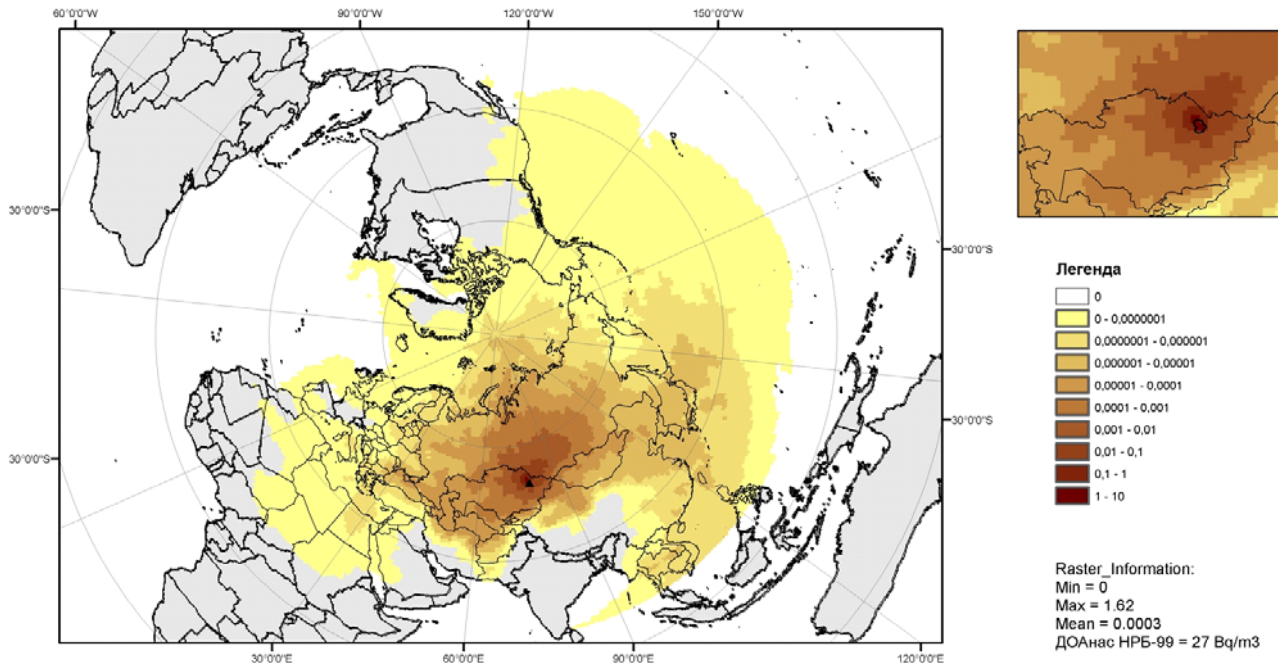


**Figure B3.** Average annual concentration of Cs-137 (Bq/m<sup>3</sup>) of radioactive pollution spreading from the epicenter located in the vicinity of testing ground Experimental Field.

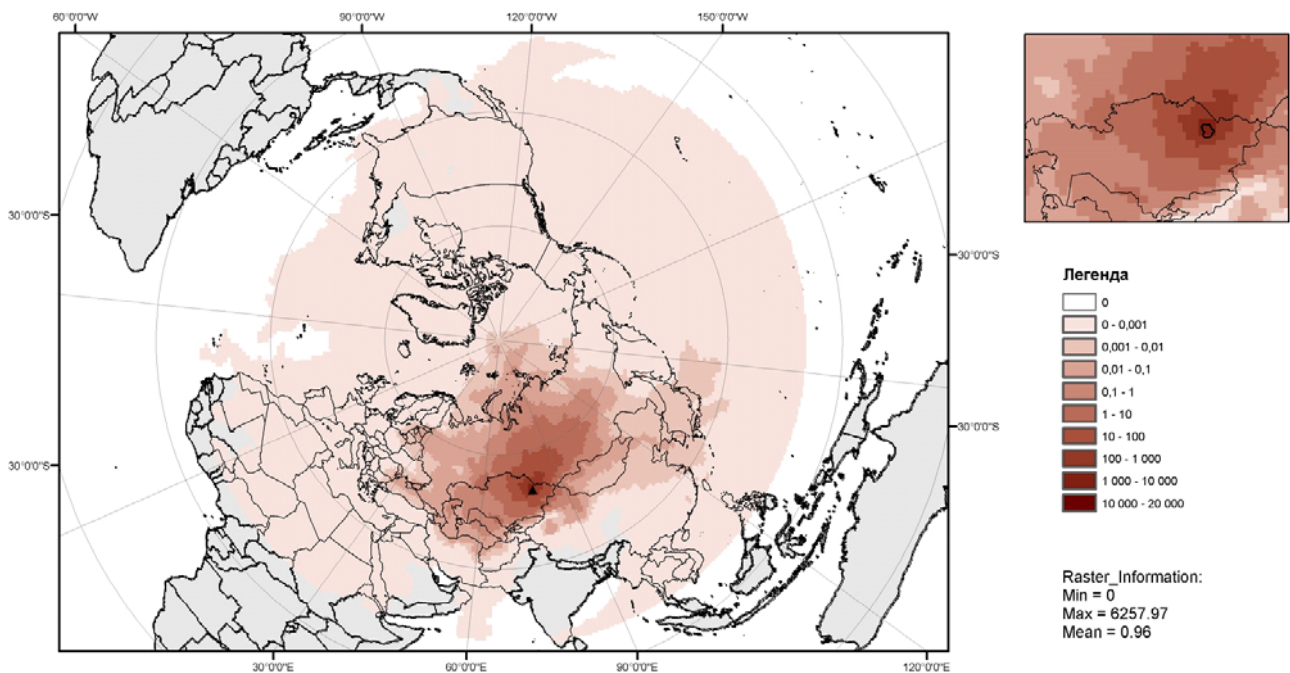


**Figure B4.** Average annual total deposition of Cs-137 (Bq/m<sup>2</sup>) of radioactive pollution spreading from the epicenter located in the vicinity of testing ground Experimental Field.